Geoenvironmental Disasters

REVIEW Open Access

Susceptibility of typical marine geological disasters: an overview

Xiaolei Liu[1,4], Yueying Wang[1], Hong Zhang[3] and Xingsen Guo[1,2*]

Abstract

Background Marine geological disasters (i.e., catastrophic events occurring in marine environments) may seriously threaten the safety of engineering facilities, life, and property in shallow- and deep-sea areas. The development of marine resources and energy and the protection of the marine geo-environment are topics of intense interest globally, and these activities inevitably require the assessment of marine geological disasters, which are receiving increasing attention from academic and industrial communities. However, as a prospective analysis for the risk assessment and management of marine geological disasters, the susceptibility of marine geological disasters, referring to a qualitative or quantitative description of the type, volume (or area), and spatial distribution of existing or potential geological disasters, is still in the exploration stage.

Results In this study, we systematically combine the theoretical basis and methods for the analysis of the susceptibility of marine geological disasters (i.e., heuristic approach, deterministic approach, and statistical approach). Taking two widely studied marine geological disasters (i.e., seabed liquefaction and submarine landslides) as examples, we review their triggering mechanism, condition factors, methodological advances, and susceptibility maps. Subsequently, some challenges in the susceptibility assessment of the marine geological disasters associated with seabed liquefaction and submarine landslides and extension to other types of marine geological disasters are briefly summarized and discussed, involving an incomplete evaluation system, poor applicability of methods, and insufficient databases.

Conclusion Based on a literature review using the extensive literature database, we focused on the susceptibility of two typical marine geological disasters (i.e., seabed liquefaction and submarine landslides) and systematically summarized the development history, methods, results, problems, and future directions. According to the challenges of this field, we recommend that relevant organizations focus on the construction of a susceptibility system and study the triggering mechanisms of marine geological disasters. Long-term in situ observation efforts should also be supported to obtain more data to improve the disaster inventory. Ultimately, more reliable methods can help improve the credibility and usefulness of susceptibility analysis results.

Keywords Marine geological disasters, Susceptibility, Method, Seabed liquefaction, Submarine landslides

*Correspondence:
Xingsen Guo
xingsen.guo@ucl.ac.uk
Full list of author information is available at the end of the article

Table 1 The causes of marine geological disasters (modified from Camargo et al. 2019; Ye et al. 2017b; Cuomo 2020)

Occurrence and duration time	Hazard factor				
	Natural genesis				Human genesis
	Tectonic activities	Gravity (slope) effect	Coastal dynamic effect	Erosion accumulation effect	
Burst type	Earthquakes, Tsunami, Landslides and liquefaction, Fault activities, Ground fissure, and Volcanic activities	Collapse, Landslide, Debris flow, Submarine turbidity current, and Land collapse	Tsunami, storm surge	Sudden estuary and harbor siltation	Harbor and waterway sudden siltation, Rock burst, Water inrush, and artificially induced earthquake
Gradually varied type	Ground deformation, Block displacement, and Crustal movement	Ground deformation	Coastal erosion, Seawater intrusion, and Sea level rise	Coastal erosion, Estuary and harbor siltation, Sluice siltation, and Tidal sand ridge	Seawater intrusion, Land subsidence, Coastal erosion, and Harbor and waterway siltation

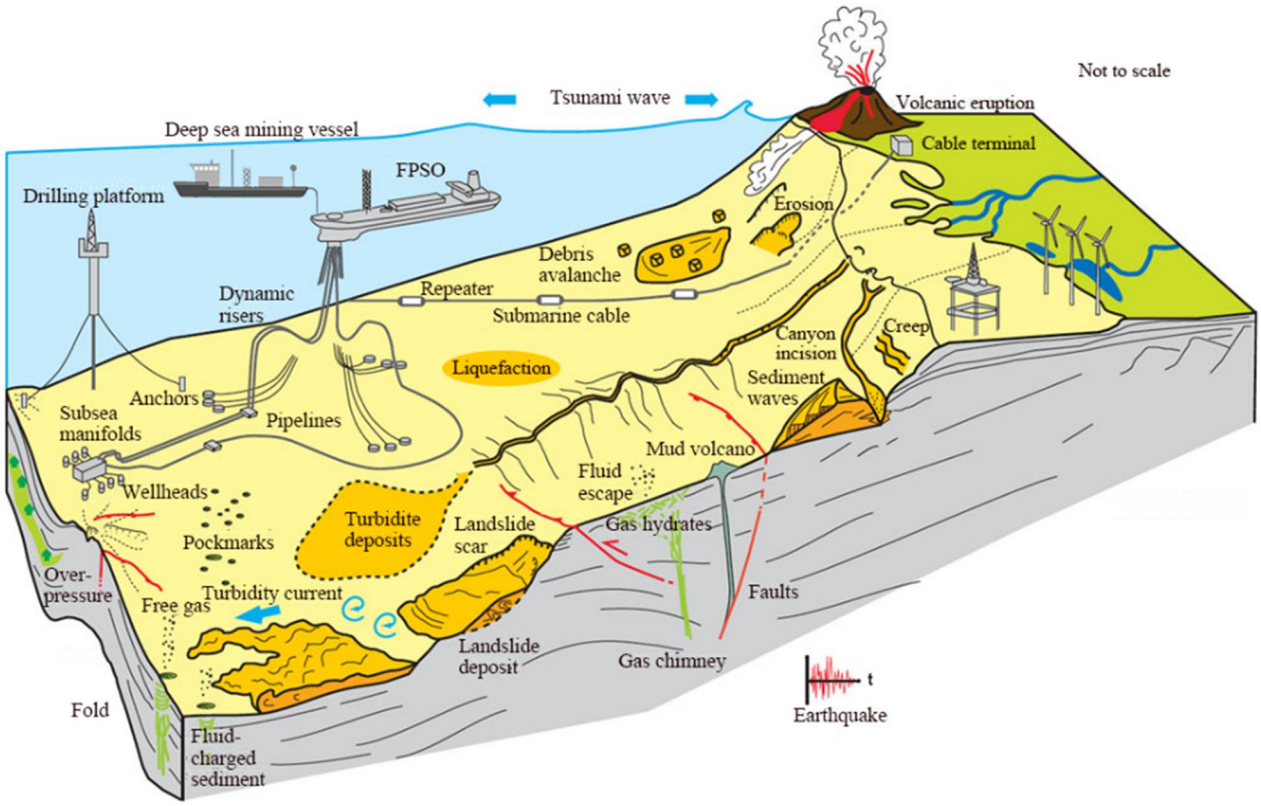

Fig. 1 Cartoon summarizing the seafloor features linked to potential geological disaster processes. This figure shows an idealized continental margin with both natural geohazard-bearing features and major anthropogenic structures lying on the seafloor (modified from Chiocci et al. 2011)

Introduction

Marine geological disasters refer to catastrophic events that occur in marine environments caused by all kinds of natural geological processes and human activities during the evolution of the Earth, including earthquakes, volcanoes, shallow-layer high-pressure gas, submarine landslides, and liquefaction, as shown in Table 1 (Camargo et al. 2019; Ye et al. 2017a). Figure 1 presents some typical marine geological disasters. Large-scale and destructive seabed liquefaction and submarine landslides have posed a threat to the safety of engineering facilities, life, and property in shallow- and deep-sea areas and are receiving increasing attention from academic and industrial communities (Jia

et al. 2016; Liu et al. 2020; Yu et al. 2023). For instance, there have been 7 wellhead and platform tip-overs, 17 submarine cable failures, and 2 submarine pipeline breaks in the Chengdao area of China caused by seabed liquefaction in the past 20 years. In 2018, a tsunami caused by a submarine landslide occurred in the Sunda Strait in western Indonesia and left nearly 500 people dead or missing and more than 1400 injured (Liu et al. 2019, 2021; Wen et al. 2019; Zhang et al. 2020).

To effectively predict and evaluate the occurrence probability and harm degree of marine geological disasters, risk analysis has been widely studied. To better understand the knowledge evolution, research hotspots and frontiers in this field, literature mining of publications on the risk analysis of marine geological disasters from January 2002 to January 2023 was conducted using the Web of Science Core Collection database and the Science of Citation Index Expanded (SCIE) bibliographic database. We analyzed the keywords of nearly 300 relevant articles which met the study criteria by CiteSpace (version 6.1.R6) (Yang et al. 2022; Reichenbach et al. 2018). Figure 2 presents co-occurrence analysis of keywords on the risk analysis of marine geological disasters. Those keywords can be roughly divided into three categories, i.e., "Methods", "Risk analysis" and "Marine geological disasters". Studies on risk analysis of marine geological disasters pays more attention to the evaluation method. Susceptibility, as a basic step of risk analysis, has been continuously developed. In terms of disaster types, researchers mainly focus on submarine landslides, earthquakes, seabed liquefaction, and sediment instability. Figure 3 presents the distribution of submarine landslides at a global scale. Submarine landslides have the characteristics of wide distribution, large scale, high degree of hazard, and frequent occurrence (Guo et al. 2019; Shan et al. 2022). Evidently, based on the temporal and spatial characteristics of marine geological disasters associated with seabed liquefaction and submarine landslides, it is necessary to carry out susceptibility assessments (i.e., for addressing the susceptibility of potentially impacted targets to the spatial component of marine geological disasters), and such assessment results are a significant basis for construction site selection, early warning, and postdisaster reconstruction (Avdievitch and Coe 2022; Maloney et al. 2020).

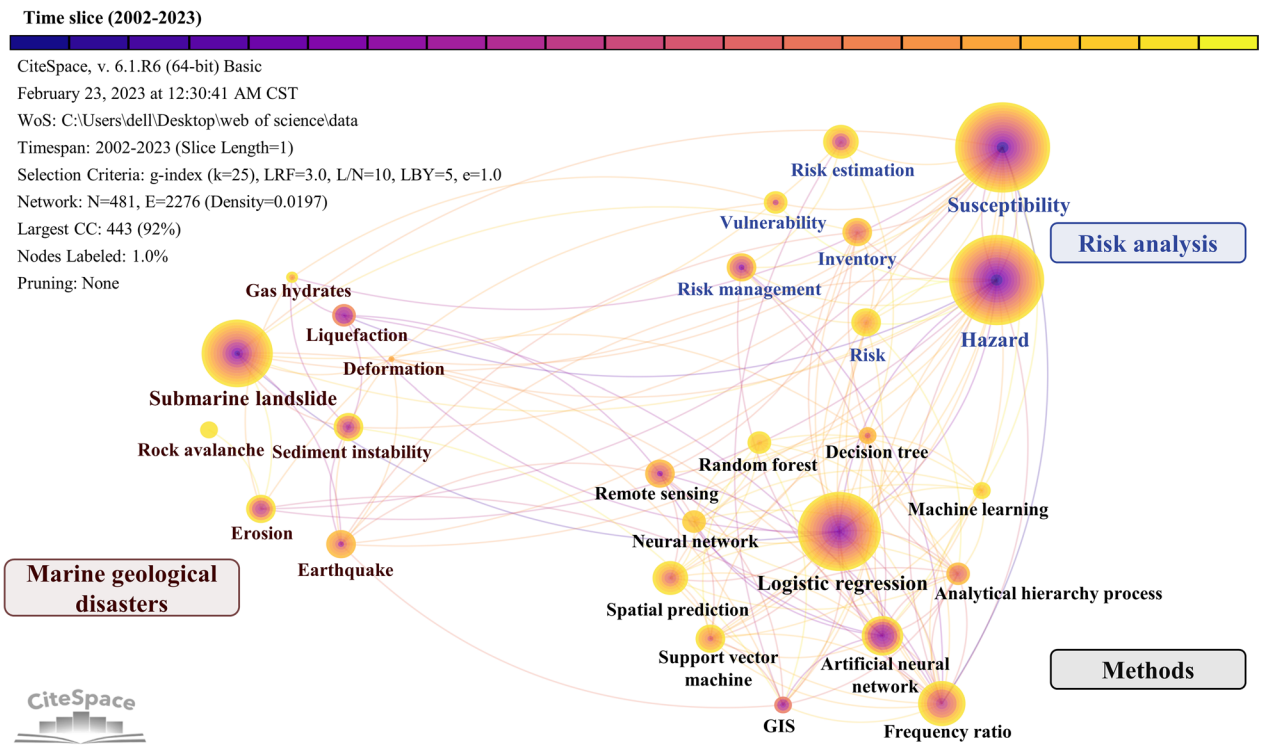

Fig. 2 Co-occurrence analysis of keywords on the risk analysis of marine geological disasters from 2002 to 2023. The circles are the nodes of keywords, the size of a circle represents the frequency of the word, the change in color from the center to the outer edge represents the change in word frequency over time (data from Web of Science™); where the retrieval strategy consisted of searching for the topics "susceptibility*" or "hazard*" or "risk*" AND "assessment*" or "evaluation*" AND "marine" or "submarine" or "ocean" or "sea*" AND "geolog*" or "geotechni*", and the asterisk (*) represents any group of characters, including no character

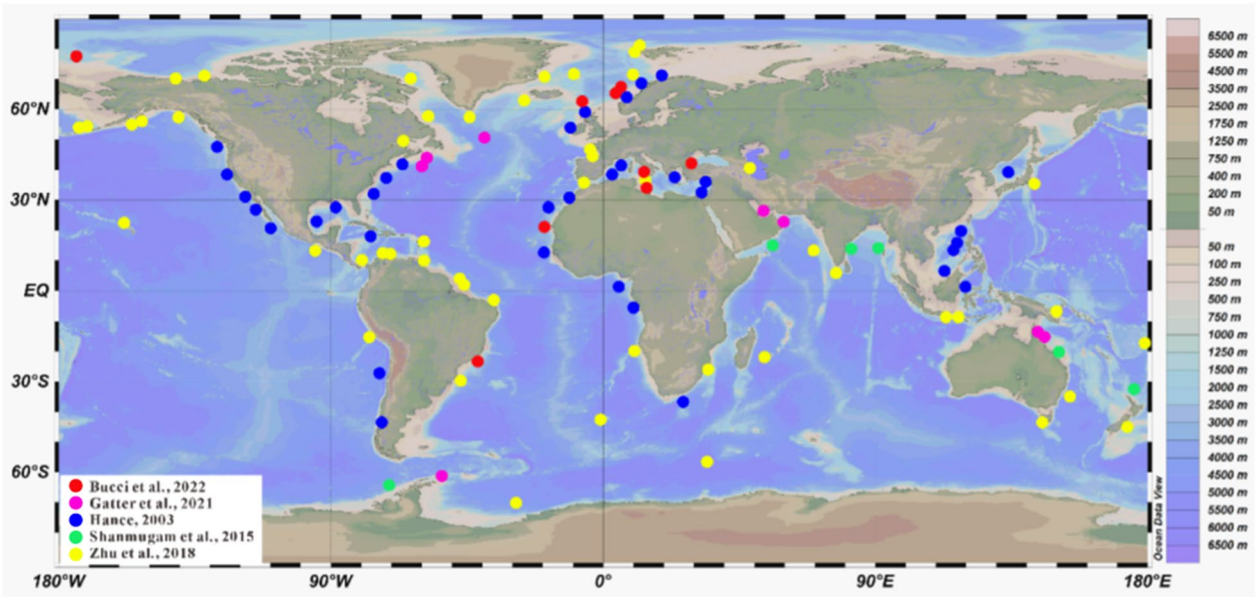

Fig. 3 Worldwide distribution of major submarine landslides (data from Bucci and Tuttleb 2022; Gatter et al. 2021; Hance 2003; Shanmugam and Wang 2015; Zhu et al. 2018)

Since the 2000s, some academics have started to study the susceptibility of marine geological disasters. Locat and Lee (2002) integrated mass movement mechanics into the evaluation of marine geological disasters to develop and perform proper risk assessment for human activities offshore. Mitchell (2003) first reported the susceptibility of marine geological disasters (i.e., mid-ocean ridge volcanic islands and seamounts to large-scale landslides), which promoted research and application progress in the field of geological disaster risk assessment. Hitchcock et al. (2010) developed a GIS-based approach for delineating the relative susceptibility of underwater slopes to mudflows. Based on the digitization and analysis of available bathymetric and geological map data, the susceptibility of the Mississippi Delta to mudflows was mapped, and it was the first geographic information system (GIS) to be applied to susceptibility. León et al. (2011) applied the bivariate statistical method to the susceptibility of seafloor features related to fluid flow from crater-like depressions and submarine landslides on the Iberian margin of the Gulf of Cádiz, which was the first time that the statistical approach was applied to the marine geological disaster susceptibility. In the context of increasing requirements for marine resources and construction protection, relevant industries are paying great attention to marine geological disaster susceptibility, which is still in the exploratory stage, mainly due to some limitations, such as an incomplete evaluation system, poor applicability of methods, and insufficient data (Chiocci et al. 2011). Therefore, we synthesize existing studies on the susceptibility of two typical marine geological disasters (i.e., seabed liquefaction and submarine landslides) to provide some recommendations for the selection, use of susceptibility methods and associated susceptibility maps, and summarize the existing problems and future development directions.

The remainder of this study is organized as follows. In "Background" section, background information on susceptibility analysis methods is systematically presented. In "Susceptibility of seabed liquefaction" and "Susceptibility of submarine landslides" sections, the susceptibility of seabed liquefaction and submarine landslides is discussed in detail in terms of triggering mechanism, condition factors, and susceptibility maps. In "Future challenges" section, the main remaining challenges and future perspectives of marine geological disaster susceptibility are highlighted. The summary and conclusions are presented in "Conclusions" section.

Background

General concepts

A susceptibility assessment system was developed in 2008. The Joint Technical Committee on Landslides and Engineered Slopes (JTC-1) combined the work of the International Society for Soil Mechanics and Geotechnical Engineering (ISSMGE), the International Society for Rock Mechanics (ISRM), and the International Association for Engineering Geology and the Environment (IAEG) to standardize the risk assessment system of landslides, which clarified the definition of risk

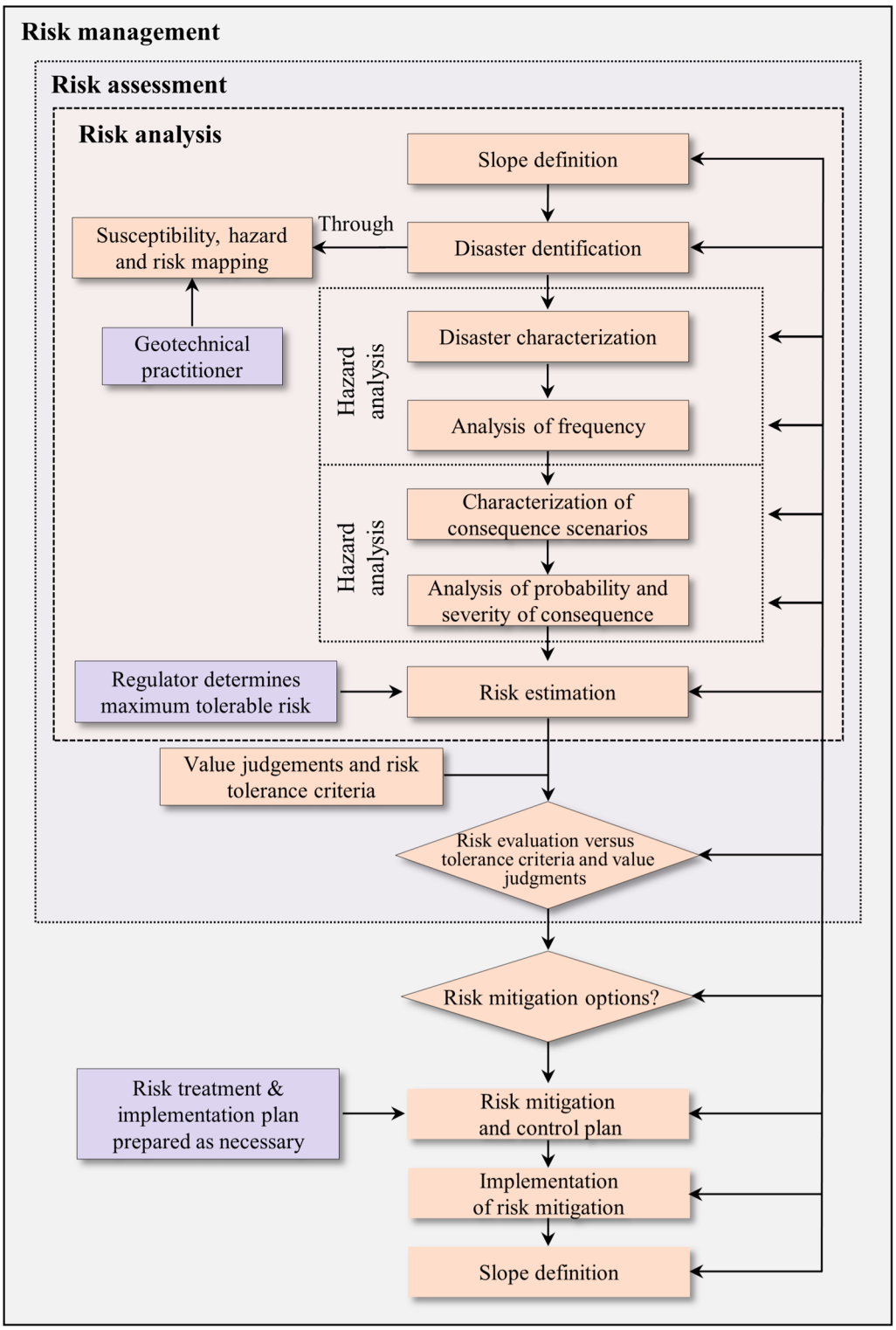

Fig. 4 Geological disaster risk analysis and management flow chart (modified from Fell et al. 2008)

assessment of geological disasters and explained the conditions and influencing factors to be considered when assessing the risk of landslides (Fell et al. 2008; Xu et al. 2015; Lukasz and Joanna 2021; Cao et al. 2022), as shown in Fig. 4. Risk assessment is a subset of risk management and is combined with risk analysis, risk estimation, and risk evaluation. Susceptibility, hazard and risk belong to the risk analysis.

Susceptibility is a quantitative or qualitative assessment of the classification, volume (or area) and spatial distribution of a geological disaster that exists or potentially may occur in an area (Xu et al. 2015, 2022). Hazard represents the probability of the occurrence of a geological disaster within a given period. Risk is a measure of the probability and severity of an adverse effect on health, property or the environment (Fell et al. 2008). The definitions of susceptibility and hazard are often confused. We note that hazard refers to the probability of geological disasters occurring within a given period. In addition to predicting where geological disasters will occur, geological disaster hazard assessments predict when or how frequently they will occur and how large they will be, which is the biggest difference between these two definitions (Shano et al. 2020). Risk assessment emphasizes the impact of disasters on society. The assessment results of the three are increasingly in line with the actual situation, which is a progressive process (Lacasse et al. 2019). As the first and key step of risk analysis, susceptibility mainly includes the establishment of a disaster inventory, the selection of condition factors and the identification of assessment methods. It directly determines the accuracy of the risk assessment, and the evaluation results are mostly presented in the susceptibility zoning map (Gamboa et al. 2021; Xu et al. 2015; Zhang et al. 2022).

Approaches for susceptibility

Many methods have been applied to the susceptibility of terrestrial geohazards, but only the following three are widely applied to marine geological disasters: (1) heuristic approach, (2) deterministic approach, and (3) statistical approach (Marques et al. 2013).

Heuristic approach

Heuristic approaches, such as the analytic hierarchy process (AHP), are indirect and qualitative methods with requirements for data based on prior insight into the causes and instability of geological disasters in the investigation area (Saaty 1990). The AHP assigns the weight of factors by the comparison matrix (Zare et al. 2022). It builds by comparing each pair of condition factors, as shown in Fig. 5. Using the AHP in susceptibility analysis involves three steps: (1) creating an evaluation hierarchy that contains target and indicator layers; (2) constructing a comparison matrix to realize a pairwise comparison of condition factors and assign relative weights to each factor, as shown in Table 2; and (3) normalize the principal eigenvector vector and calculate the weights of each condition factor (Saaty 1990). The random consistency index (CI) and the random consistency ratio (CR) are calculated to assess whether the construction of the comparison matrix and

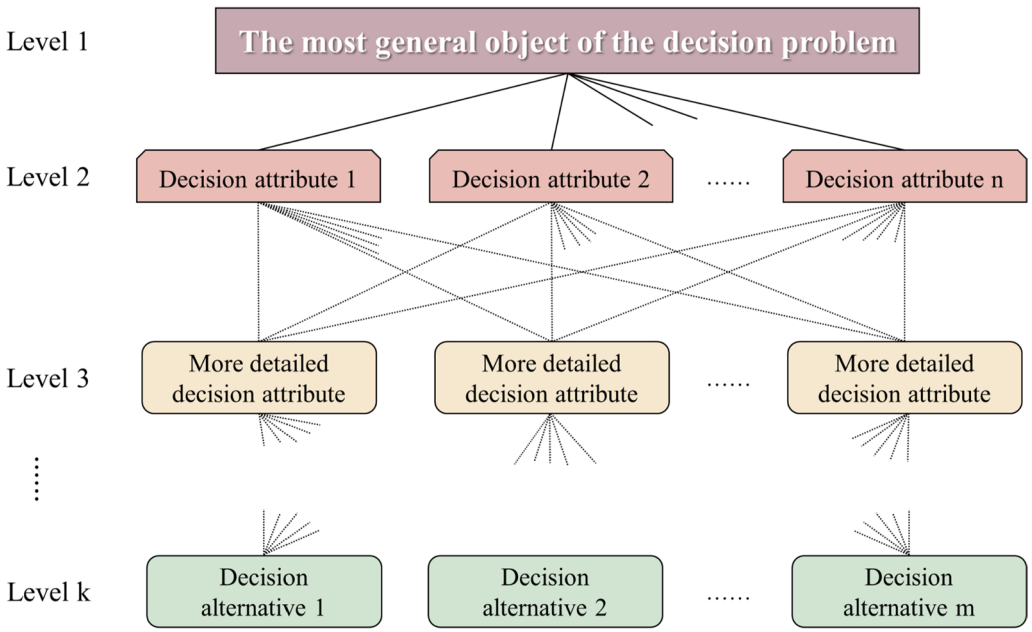

Fig. 5 Form of decision elements in the AHP (modified from Zahedi 1986)

Table 2 The scale and its description (modified from Saaty 1977)

Preference factor	Degree of preference	Explanation
1	Equally	These two factors contribute equally to the objective
3	Moderately	Experience and judgment slightly to moderately favor one factor over another
5	Strongly	Experience and judgment strongly or essentially favor one factor over another
7	Very strongly	The analytic hierarchy process: planning, priority setting, resource allocation
9	Extremely	The evidence of favoring one factor over another is of the highest degree possible of an affirmation
2,4,6,8	Intermediate	Used to represent compromises between the preferences in weights 1, 3, 5, 7 and 9
Reciprocals	Opposites	Used for inverse comparison

the relative weights of the condition factors are reasonable (Zahedi 1986). The selection of the random matrix consistency index (RI) is based on the research field and the relationship of condition factors. The CI value is associated with the maximum characteristic root of the comparison matrix, as given in Eq. (1). The smaller the CI value is, the closer the comparison matrix is to consistency. The CR value is related to the CI value and the order of the comparison matrix, as given in Eq. (2).

$$CI = \frac{\lambda_{\max} - n}{n - 1} \tag{1}$$

$$CR = \frac{CI}{RI} \tag{2}$$

where n is the number of condition factors (Zare et al. 2022).

The accuracy of the result depends on the available information, so it is suitable for small and medium scales. This method has been applied to the susceptibility of submarine landslides at present, as detailed in "Advances in the susceptibility of submarine landslides" section.

Deterministic approach

The deterministic approach is a quantitative assessment method for geological disasters in large-scale geological disasters (Locat and Lee 2002). It is based on comprehension of the occurrence mechanism of marine geological disasters and their physical laws (Collico et al. 2020; Zhou et al. 2021). The safety factor is defined as the ratio of the resistance to the driving force, as given in Eq. (3).

$$F = \frac{\sum Resisting\ Forces}{\sum Gravitational\ Forces} \tag{3}$$

For seabed liquefaction, two main approaches of the deterministic approach applied in the susceptibility of seabed liquefaction are as follows. (1) Effective stress discrimination: When the internal excess pore water pressure of the sediment is greater than the overlying effective stress, it becomes liquefied, as given in Eq. (4):

$$\sigma_v' = \sigma_{v0}' - P_e \tag{4}$$

where σ_v' is the effective stress; σ_{v0}' is the vertical effective stress of sediment under static water conditions; and P_e is the wave-induced excess pore pressure. The closer the value of P_e/σ_{v0}' is to 1, the more likely the sediment is be unstable. (2) Shear stress coefficient method: When the wave-induced shear stress is greater than the capacity of the sediment to resist liquefaction, the sediment becomes liquefied. The critical cycle stress ratio response to sediment liquefaction (Seed and Izzat 1971) is given in Eq. (5):

$$FS_{liquefaction} = \frac{CRR}{CSR} \tag{5}$$

where CRR is the cyclic resist resistance ratio and CSR is the cyclic stress ratio. The closer $FS_{liquefaction}$ is to 1, the more likely the sediment is be unstable.

For submarine landslides, stability evaluation is usually carried out based on the safety factor using the ratio of the shear strength and downward sliding (Liu et al. 2018). For instance, Ikari et al. (2011) quantified the likelihood of slope sediment failure using a one-dimensional infinite slope factor of safety model, as given in Eq. (6):

$$F = \frac{\tau_i}{\left(\sigma_v' cos\theta sin\theta\right) + S} \tag{6}$$

The establishment of the safety factor relies on the geological environmental conditions and external loading in the study area, which will be presented in "Advances in the susceptibility of submarine landslides" section.

The input and output parameters in the deterministic approach are easy to understand, but this method is too fixed to handle the uncertain relationship between the operational model and the data, and the method lacks universality. Ulker and Rahman (2009) evaluated three dynamic cases by equation derivation and numerical

simulations based on the dynamic response of different properties of the seabed to wave loads. There is a certain gap in the simulation results of different methods for the same seabed.

Statistical approach

A statistical approach can be used for the qualitative and quantitative evaluation of geological disasters based on statistical principles to describe the correlation between condition factors. Accordingly, this method, including bivariate statistical analysis, multivariate statistical analysis, and machine learning (neural network model and maximum entropy model), is broadly utilized in the susceptibility analysis of marine geological disasters.

(1) Wi-index bivariate analysis (Fig. 6) is a bivariate analysis technique that is mainly used in the risk assessment of marine geological disasters. Considering the relationship between the distribution density of the disaster in different classes of condition factors and in the study area, the Wi-index can be calculated by relative weights of different levels in each condition factor and presented in a susceptibility map. This method applies to the susceptibility of large-scale geological disasters, and the formula is shown in Eq. (7) (Van Westen 1997).

$$W_i = ln\left[\frac{Densisty\ Class}{Densisty\ Map}\right] = ln\left[\frac{Area(Si)/Area(N_i)}{\sum Area(Si)/\sum Area(Ni)}\right] \tag{7}$$

The final W_t value is obtained by summing the W_i value of each condition factor, as given in Eq. (8):

$$W_t = \sum W_i \tag{8}$$

where W_t is the susceptibility of geological disasters; W_i is the weight assigned to a specific parameter; *Density Class* is the density of the parameter class; *Density Map* is the disaster density for the whole map; $Area(Si)$ is the area affected by landslides in the factor map; and $Area(Ni)$ is the surface of a class in the factor map. Although the bivariate statistical analysis method is a quantitative method, this technique is subjective, and it is difficult to gauge whether there is a high correlation between the selected condition factors and the event (Mersha and Meten 2020).

(2) Multivariate Statistical Analysis. This method can build a multifactor relationship network to generate the disaster evaluation results of an area based on sufficient data and cases of geological disasters (Guzzetti et al. 2005). The logistic regression (LR) method, which is a multivariate statistical approach, is a variable analysis model applicable to the study of susceptibility at small and medium scales and has been applied to the susceptibility analysis of submarine landslides. In terms of different categories of dependent variables and their values, the method can be divided into the binomial logistic regression method and the multivariate logistic regression method (Guzzetti et al. 2005; Guzzetti 2006). The binomial logistic regression method can predict the relationship between a dichotomic dependent variable (0 without instabilities, 1 with instabilities) and a set of independent explanatory variables (predisposing factors) (Rasyid et al. 2016). The correlation between the occurrence of a geological disaster and the condition factors is expressed as shown in Eq. (9).

$$S = \frac{1}{1+e^{-\psi}} 0 \le S \le 1 \tag{9}$$

where S (from 0 to 1) is the probability of a given terrain being in the group of the units affected by instabilities and ψ is the logit, which is linearly related to the independent variables, as given in Eq. (10):

$$\psi = \log\left(\frac{P}{1-P}\right) = \beta_0 + \beta_1 x_1 + \ldots + \beta_m x_m + \varepsilon \tag{10}$$

where P is the possibility of the occurrences of an event; β_0, β_1,..., β_m are the slope coefficients of the logistic regression model; x_1, x_2,..., x_m are the independent variables; and ε is the error associated with model fitting (Can et al. 2005; Lee 2004).

This method does not need to consider the influence of weight, and its condition factors can be continuous or discrete and subject to historical data. Thus, for areas with abundant historical data, the LR method is more accurate.

(3) With the growth of artificial intelligence, machine learning methods, such as artificial neural network models (Fig. 7), have been applied in the marine geological disaster susceptibility analysis (Mandal et al. 2008). This method simplifies the problem in the form of multiple interconnected neurons, and each neuron model consists of input layers, hidden layers, and output layers (Aleotti et al. 1999). This method can be used to address nonlinear problems with complex variables, ambiguous functional relationships or unclear relationships among influencing factors.

The maximum entropy model (MaxEnt) is a statistical machine learning approach that is currently applied to the susceptibility analysis of submarine landslides (Phillips et al. 2006). It considers the model with the highest entropy among all probability models as the result of the mid-evaluation, following the principle of modeling the known information and making no assumptions about the unknown information (Phillips

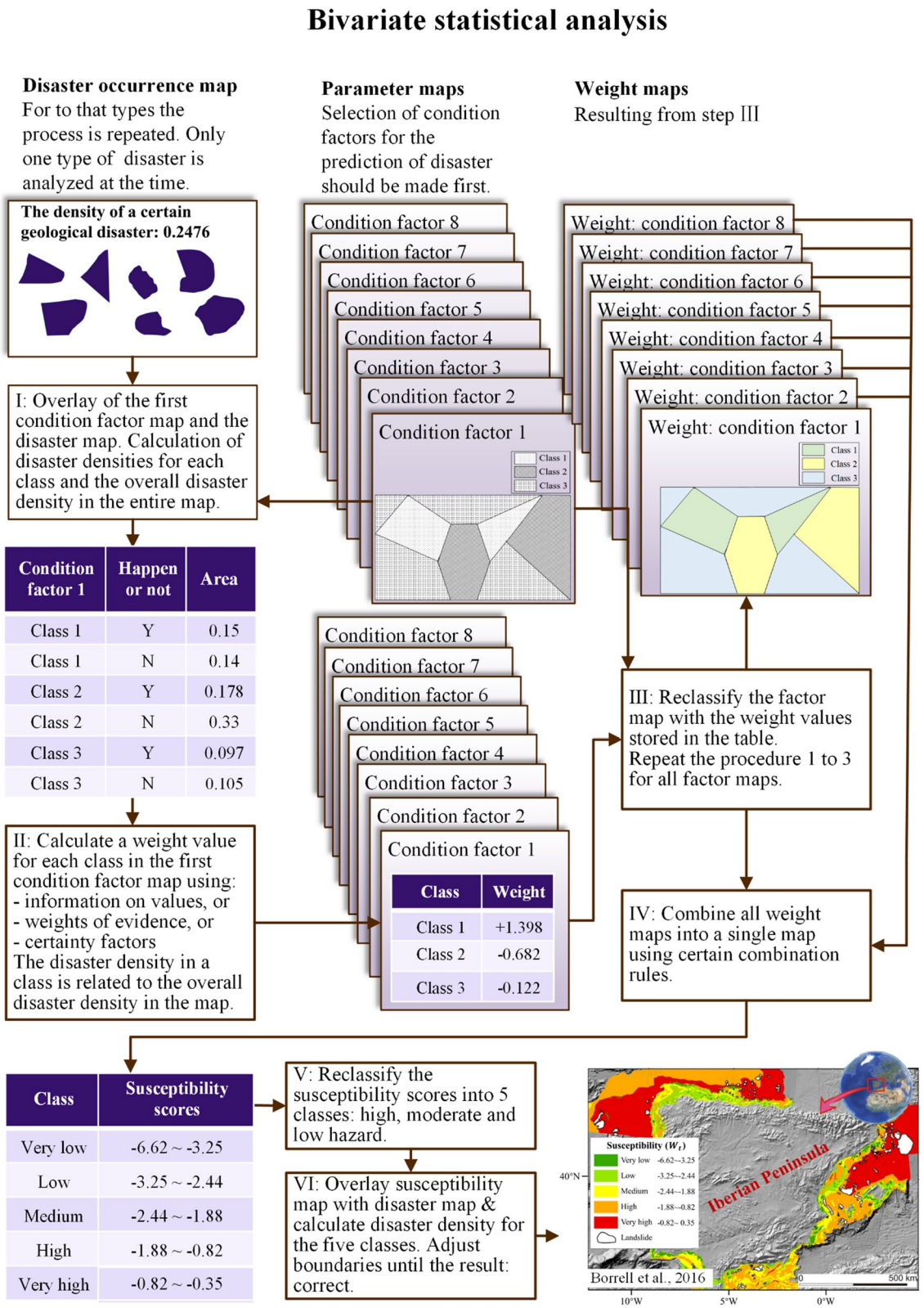

Fig. 6 Bivariate statistical analysis method (modified from Van Westen 1997)

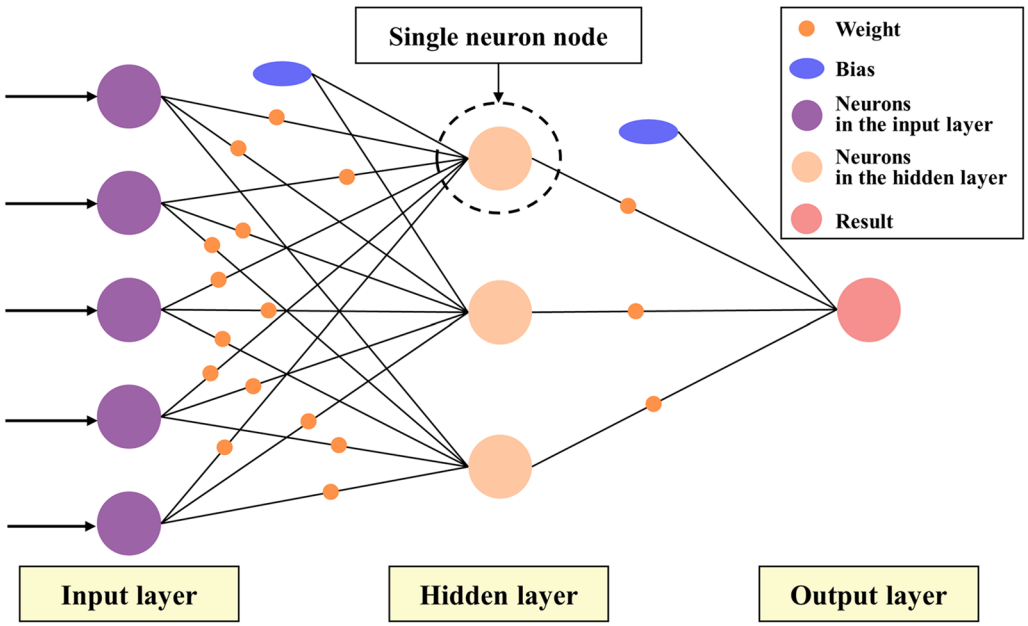

Fig. 7 Artificial neural network model (modified from Aleotti et al. 1999)

et al. 2008). The set of Models C that satisfies all constraints is shown in Eq. (11):

$$C \equiv \left\{P \in P | E_p(f_i) = E_{\tilde{P}}(f_i), i = 1, 2, \ldots, n\right\} \quad (11)$$

The conditional entropy defined by the conditional probability distribution $P(Y|X)$ is shown in Eq. (12):

$$H(P) = -\sum_{x,y} \tilde{P}(x) P(y|x) \log P(y|x) \quad (12)$$

where the entropy maximum model H(P) that satisfies the condition is called the maximum entropy model.

MaxEnt allows a more complete study of the susceptibility in a study area. Felicísimo et al. (2013) compared several susceptibility methods and concluded that MaxEnt was one of the methods with optimal evaluation results, although it was rarely applied to submarine landslides.

Susceptibility mapping of marine geological disasters

The abovementioned methods for measuring susceptibility have been systematically classified, but some of them, such as deterministic methods, can only reflect the susceptibility of sampling points in the study area. It is difficult to realize the susceptibility of geological disasters over the whole study area (Budetta et al. 2008; Zhu et al. 2018). The data processing and analysis tools in GIS have been used to partition the susceptibility of the whole area as people build geographic information systems. Spatial interpolation, as an efficient statistical tool for spatial information, has been widely exploited by researchers (Al-Umar et al. 2020).

Spatial interpolation is a GIS data processing and analysis tool used to convert data from discrete points to continuous planes (Wang et al. 2005). To rebuild the continuous geographic phenomena, limited sampling data is used to estimate attribute values of any data points in study area. Interpolation function ($f : x \rightarrow x$) is established by finite sampling points set ($S = \left\{(x_i, f_i), i = 1, 2, 3, \ldots, n\right\}$) in spatial interpolation (Li et al. 2015). According to the principle of the method, spatial interpolation techniques can be divided into geostatistical interpolation and deterministic interpolation (Wen et al. 2022). Among the commonly used spatial interpolation models, kriging and its variants belong to geostatistical interpolation deterministic interpolation. Inverse distance weighted (IDW), spline curve (SC) interpolation, radial basis function (RBF) and global/local polynomial (GPI/LPI) interpolation are deterministic interpolations (Hadi et al. 2018). Because research on marine geological disasters is subject to the difficulties of monitoring and a limited amount of data, kriging and IDW are most commonly applied in this field. Kriging, known as the spatial covariance optimal interpolation method, is based on variogram and structural analysis, maximizes the use of spatial information of every sampling point and integrates the size, shape and spatial orientation of the known samples to estimate the unknown samples (Hutchinson 1993). It can be divided into simple kriging, ordinary kriging, universal kriging, cokriging,

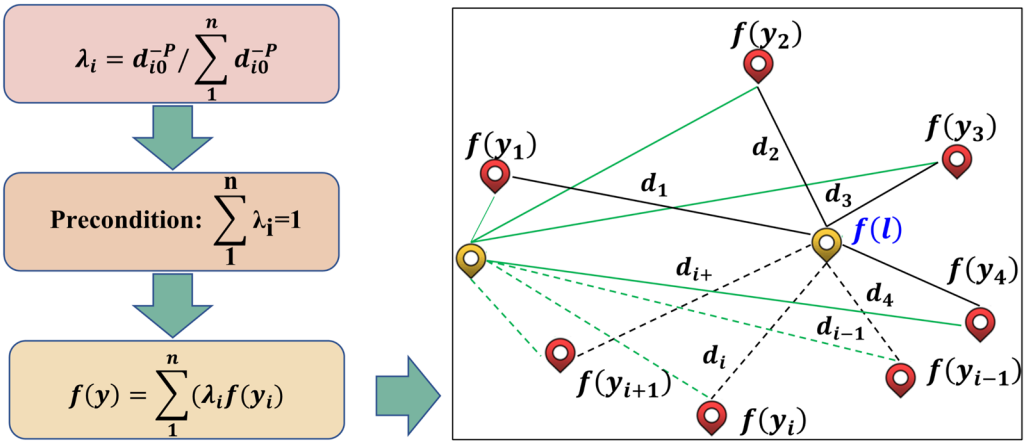

Fig. 8 Inverse distance weighted interpolation theory (modified from Nian et al. 2019)

Bayesian kriging and disjunctive kriging (Babak et al. 2009; Kleijnen 2009). IDW is defined as the spatially weighted average of sample values within the study area. That is, the distance between the interpolation point and the sample point is used as a weight. The closer the sample point is to the interpolation point, the greater the weight given to the sample point (Bokati et al. 2022). Figure 8 shows the process of IDW. d_i is the distance of two points. λ_i is the distance weight. $f(l)$ is the measured value and the value of $f(y)$ is based on the calculation by IDW. However, there is no absolute best method for spatial interpolation. To obtain the ideal spatial interpolation effect, method selection should be based on the study purpose and consideration of the pros and cons of each method (Nian et al. 2019). Although IDW has great operability and robustness, it has requirements for the density of known samples and the dispersion of their distribution. IDW may be superior to kriging when the study area has a small database (Wen et al. 2022). In contrast, kriging not only refers to the spatial characteristics

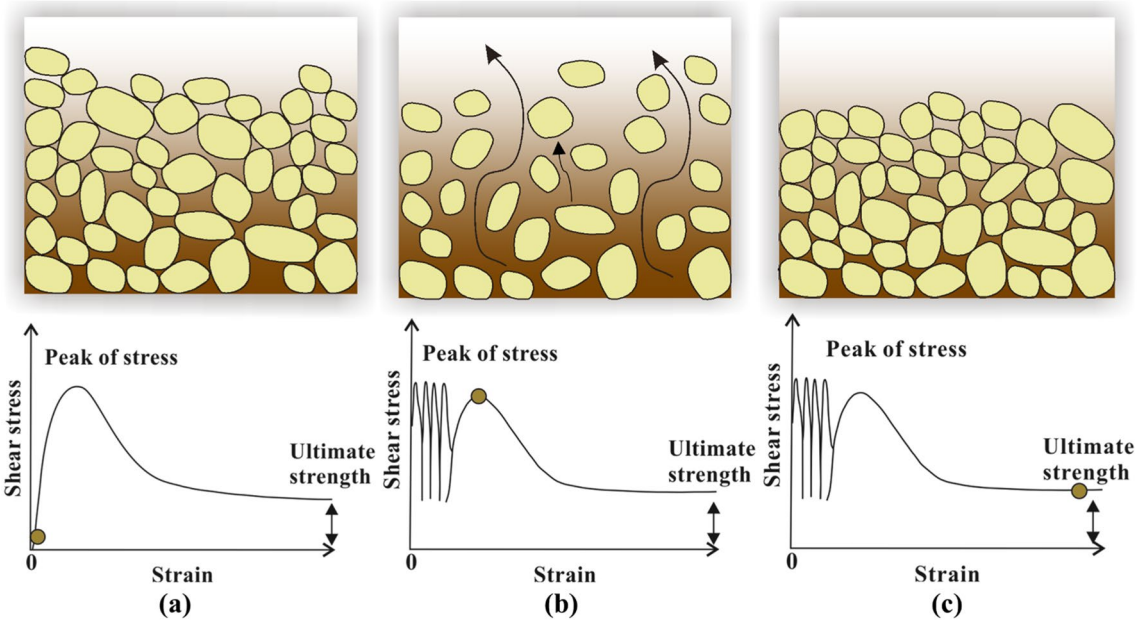

Fig. 9 Liquefaction process. The orange dot on the stress–strain curve indicates the stage of the process illustrated in the diagram above: **a** a potentially liquefiable sandy deposit and a hypothetical shear stress/strain curve; **b** sediment during the liquefaction process; and **c** following the earthquake and liquefaction, grains re-establish their intergrain contacts (rebuilding their effective stress), where σ´ is the total stress, σ is the effective stress and u is the pore-water pressure (modified from Bucci et al. 2022)

of the sample but also uses the coefficient of variation to describe the structure and randomness of regional variables, and the spatial distribution of the sample has less influence on the interpolation results than in IDW (Curtarelli et al. 2015; Wang et al. 2011).

Susceptibility of seabed liquefaction

Mechanism analysis of seabed liquefaction

Liquefaction is a phenomenon of sediment instability. As shown in Fig. 9, the process of liquefaction can be divided into 3 stages. Under the action of an external load, the internal stress state of the sediment changes, i.e., when the excess pore pressure is equivalent to the effective stress of the overlying sediment, the state of the sediment changes from solid to fluid, and the sediment becomes unstable (Youd et al. 1978; Jia et al. 2014). Liquefaction of the seabed can lead to the loss of strength and stiffness of the sediment, and the seabed can no longer withstand external forces, which can cause a series of engineering safety problems and pose a threat to the stability of marine engineering (Liu et al. 2022; Youd et al. 2001).

External loading conditions and substrate conditions should be considered when discussing the occurrence of seabed liquefaction, which is directly driven by external loading (Bucci et al. 2022). The main external loads for seabed liquefaction are earthquakes and waves, both of which cause different mechanisms for the occurrence of liquefaction (Wang et al. 2020b). Seismic liquefaction is a mode of seabed liquefaction that occurs when the cyclic shear stress generated by an earthquake is greater than the cyclic resistance of the sediment (Ishihara 1993). Wave-induced liquefaction was first recognized and analyzed by Bjerrum (1973) when designing the foundation for deep-water structures in the North Sea. The differential loading on the seafloor by the pressure wave induces a sequence of cyclic shear stresses in the underlying sediment. If the induced shear stress exceeds the strength, a quicksand effect occurs, and external loads cannot be supported (Nataraja et al. 1983; Xu et al. 2021). As this occurs, the sediment particles in a suspended state may be readily transported as a fluid, which may cause a vertical movement of sediment. Significant deformation or liquefaction failure may occur, thereby exerting damaging influences on nearby engineering installations (Ishihara et al. 1984; Yu et al. 2022). The mode of pore water pressure variation can be further divided into transient liquefaction and residual liquefaction. Zen et al. (1990a) compared the difference between seismic liquefaction and wave-induced liquefaction, as shown in Table 3. Although wave-induced liquefaction has a long loading time due to the wave period, wave-induced liquefaction has a long duration and a great impact on the stability of surficial sediments (Liu et al. 2022). Considering that marine engineering facilities are mostly constructed in surficial sediments, this study focuses on the mechanism of wave-induced liquefaction and its susceptibility.

Condition factors of susceptibility of wave-induced liquefaction

Zen and Yamazaki (1990b) conducted a theoretical and experimental study of wave-induced oscillatory pore pressure in the poroelastic seabed. He proposed a control equation for the oscillatory pore pressure, which was verified by model tests and applied this equation to estimate the liquefaction potential of the seabed model. Wave-induced oscillatory pore pressure is related to wave conditions and substrate conditions, as given in Eq. (13):

$$p_m = F(H, L, T, m_v, k, n, \gamma_\omega, m_\omega, h, z, l, t, S_r, N_c) \tag{13}$$

Table 3 Difference between wave-induced liquefaction and seismic liquefaction (modified from Zen and Yamazaki 1990a; Sumer et al. 2007)

Difference	Earthquake-induced liquefaction	Wave-induced liquefaction
External forces	Earthquake	Wave
Loading	Cyclic shear stress	Oscillatory water pressure
Input	Base	Surface
period	Order of 1 s	Order of 10 s
Duration	Several minutes	A couple of days or weeks
Drainage condition	Undrained	Partially drained
Excess pore pressure	Positive, gradual increase	Positive and negative, oscillatory
Effective stress	Decrease	Decrease and increase alternately
Liquefaction phenomena	Occur at once	Occur transiently and repeatedly

where p_m is the oscillatory pore pressure; H is the wave height; L is the wavelength; m_v is the coefficient of volume compressibility; k is the coefficient of permeability; n is the porosity; γ_ω is the unit weight of pore water; m_ω is the compressibility of pore water, including air; h is the water depth; z is the thickness of the seabed; l is the thickness of the permeable layer; t is time; S_r is the degree of saturation; and N_c is the number of waves (Zen et al. 1990b; Zen and Yamazaki 1991). The wave height, wavelength, and wave period belong to the wave properties, and the permeability coefficient and saturation are jointly determined by the sediment properties and the pore water properties within the sediment (Bian et al. 2020; Zheng et al. 2013).

Wave conditions

A greater wave height promotes the occurrence of liquefaction. Sumer et al. (1999) found through indoor experimental studies that waves cause an increase in pore water pressure. He considered that when sinking or floating occurred in liquefied sediments, the maximum value of accumulated pore pressure in sediment increased with wave height until the wave height reached the maximum values, as shown in Fig. 10a. P is the pore pressure. γ_ω is the specific weight of water. P_{max} is the maximum value attained by accumulated pore pressure $\bar{P}$. σ_0' is the initial mean effective stress. Jeng et al. (2007) used the Laplace transform method to derive the theoretical solution for the pore water pressure growth in the seabed under wave loading and verified it using available experimental data. They found that pore water pressure is dominated by the cumulative response at higher wave heights and

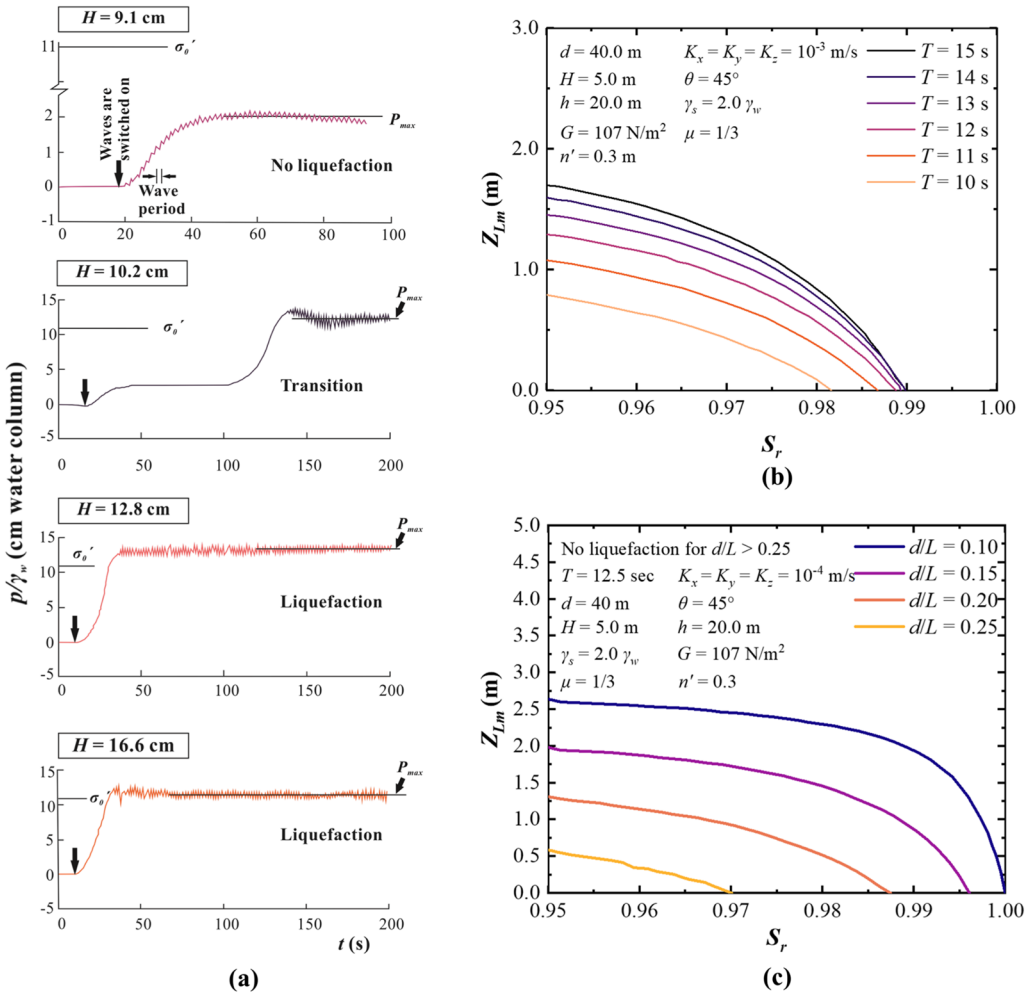

Fig. 10 Seabed liquefaction under different wave conditions: **a** wave height; **b** relative water depth; **c** wave period (modified from Jeng 2013)

the transient response at lower wave heights in shallow and transitional water depth zones. Zhang et al. (2013) derived analytical approximations for pore pressure and effective stress assessment in marine sediment under wave current loading. He found that the liquefaction depth increased significantly with increasing wave height.

The effect of the wavelength on the liquefaction degree is often measured by the relative water depth (d/L), where d is the water depth and L is the wavelength of the incident and reflected waves (Li et al. 2020). Jeng et al. (2007) investigated the degree of sediment liquefaction under different relative water depths by indoor tests and model tests and found that the maximum liquefaction depth decreased with increasing relative water depth Z_{Lm}, as shown in Fig. 10b.S_r is saturation; T is wave period; d is water depth; H is wave height; γ_s is the unit weight of sediment; γ_ω is the unit weight of water; μ is Poisson's ratio; K_x, K_y and K_z are the sediment permeabilities in the x-, y- and z- directions; θ is obliquity; h is seabed thickness; G is shear modulus; and n' is porosity. Under the same wave height, the liquefaction depth in shallow water conditions is greater than in deep water conditions, and its pore water pressure is more easily dissipated (Liu et al. 2017a; Zhang et al. 2021).

In addition, the wave period also affects the liquefaction potential of the seabed. Zen and Yamazaki (1990a) found that wave period is one of the essential factors causing the variation in pore pressure in seabed oscillation and phase lag through indoor tests. Jeng (2013) considered the effect of wave period on the liquefaction of the seabed in two dimensions, and the maximum liquefaction depth decreased with decreasing wave period, i.e., the seabed under the influence of long period waves had more potential for liquefaction, as shown in Fig. 10c. Zhang et al. (2019a) came to the same conclusion as Rahman (1991) by simulating the depth of seabed liquefaction around the foundation piles of offshore wind turbines at different wave periods.

Substrate conditions

The degree of saturation is defined as the ratio of gas volume to pore volume in sediment. The mechanical properties of sediment at different degrees of saturation depend on the micromechanical structure of the sediment skeleton, liquid, and gas (Huang et al. 2015; Li et al. 2020; Wen et al. 2019). Rahman (1991) studied various mechanisms of seabed instability caused by waves. He found that a partially saturated seabed may be liquefied by a change in the oscillating pore pressure, and the liquefaction potential of the seabed increases

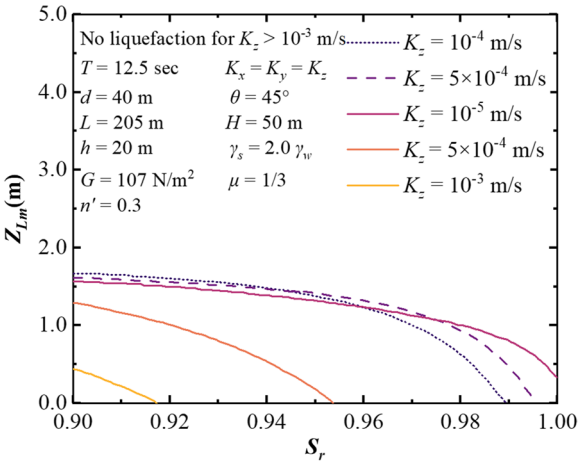

Fig. 11 Distribution of the maximum liquefaction depth Z_{Lm} versus S_r for various K_z values (modified from Jeng 2013)

with the decrease in saturation. Jeng (1997) found that the maximum liquefaction depth decreases with increasing saturation: the maximum pore pressure at $S_r = 0.975$ is almost 80% of that at $S_r = 1.0$. Liquefaction of saturated sediments occurs only in shallow-water environments with high wave heights and a very low-permeability seabed.

The coefficient of permeability K_z is used to measure the rate of fluid flow through the voids between grains, and it has the greatest influence on liquefaction. Okusa (1985) compared the mudline locations at different permeabilities through field tests and found that the lower the permeability is, the more conducive the seabed is to liquefaction. Madsen (1978) found that the variation in the permeability of seabed sediments resulted in hysteresis in the downward transmission of wave pressure. Liu et al. (2009) found that the liquefaction depth increased as the permeability decreased through model tests, while no liquefaction occurred when $K_z > 2.1 \times 10^{-4}$ ms^{-1}. Jeng (2013) found that seabed sediments were susceptible to liquefaction at $K_z = 10^{-5}$ms^{-1} through model tests, and liquefaction occurred in the $K_z = 10^{-3}$ms^{-1} seabed only when $S_r < 0.918$, as shown in Fig. 11.

Advances in the susceptibility of wave-induced seabed liquefaction

Information on the susceptibility to wave-induced seabed liquefaction is less abundant and limited to areas with a smaller average size (Lu et al. 2019). Deterministic and statistical approaches are commonly employed for seabed liquefaction susceptibility mapping. A deterministic approach is performed on the basis of safety coefficients or other discriminatory indicators for susceptibility mapping and is often accompanied by GIS for spatial

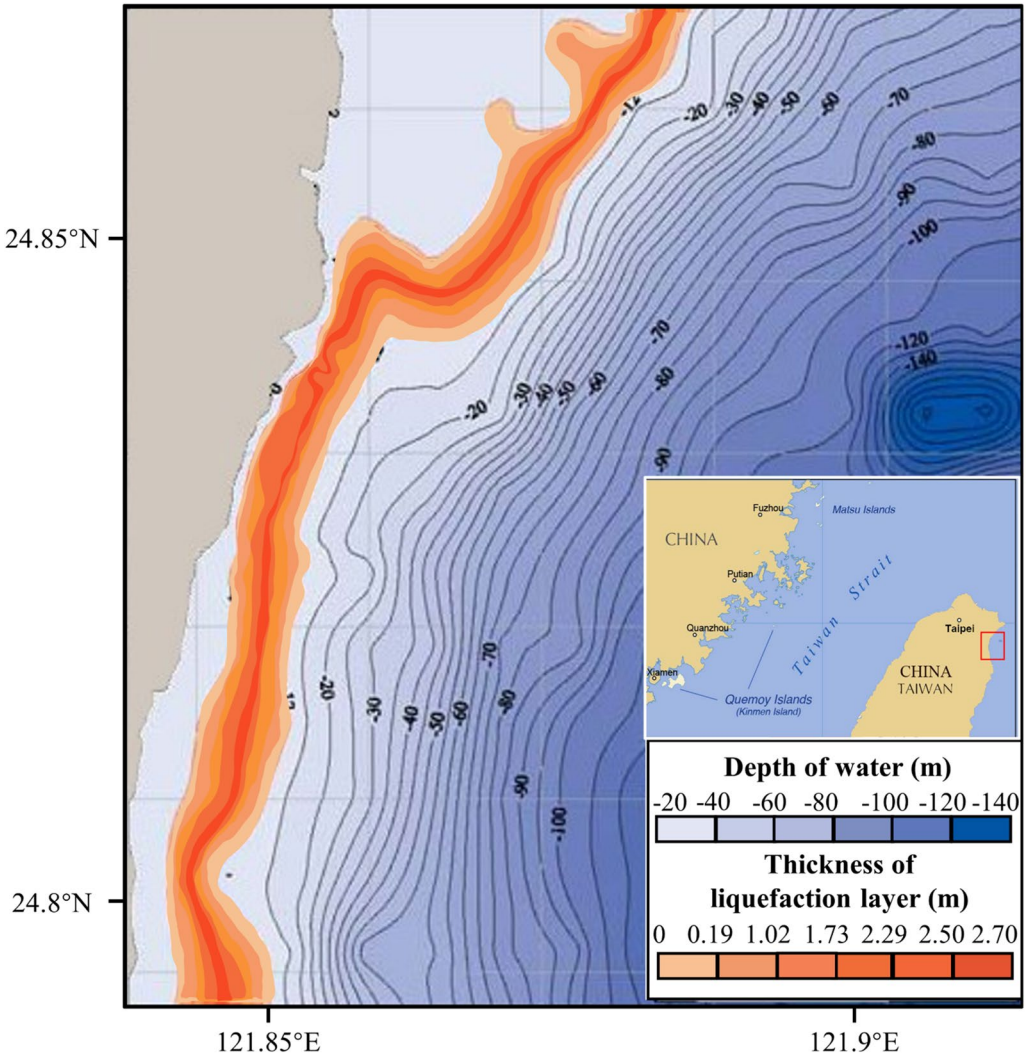

Fig. 12 The susceptibility zone map for the coastal area of Yilan, Taiwan Province, China (modified from Chang et al. 2004)

mapping. Among the statistical approaches, the most often applied are artificial neural network models.

Deterministic approach

Based on the above discriminations, the susceptibility mapping of seabed liquefaction in a study area has been driven by GIS. Chang et al. (2004) proposed a 3-D evaluation method of seabed liquefaction based on cyclic triaxial tests, liquefaction potential evaluation criteria, and the nearshore spectral windwave (NSW) model, and this method can predict the location of sandy seabed liquefaction and the thickness of the liquefaction layer, as shown in Fig. 12. The method was applied to generate a susceptibility map of the coastal area of Yilan, Taiwan Province, China. The prediction demonstrated that if a pipeline was buried at least 2.7 m below the seabed line, liquefaction would not occur even under the wave load caused by a typhoon. Nevertheless, this method did not consider the dissipation of pore water pressure during a storm surge. This result is a reference for the susceptibility assessment of shallow sediment liquefaction in a small-scale area.

Du et al. (2020) evaluated the liquefaction depth within the Chengdao Sea in the Yellow River Delta region, as shown in Fig. 13. The judgment method for excess pore water pressure was adopted to calculate the potential liquefaction depth of the seabed in different wave recurrence intervals, and the results were verified through comparison with measured sediment pore water pressure values. The smallest value between the

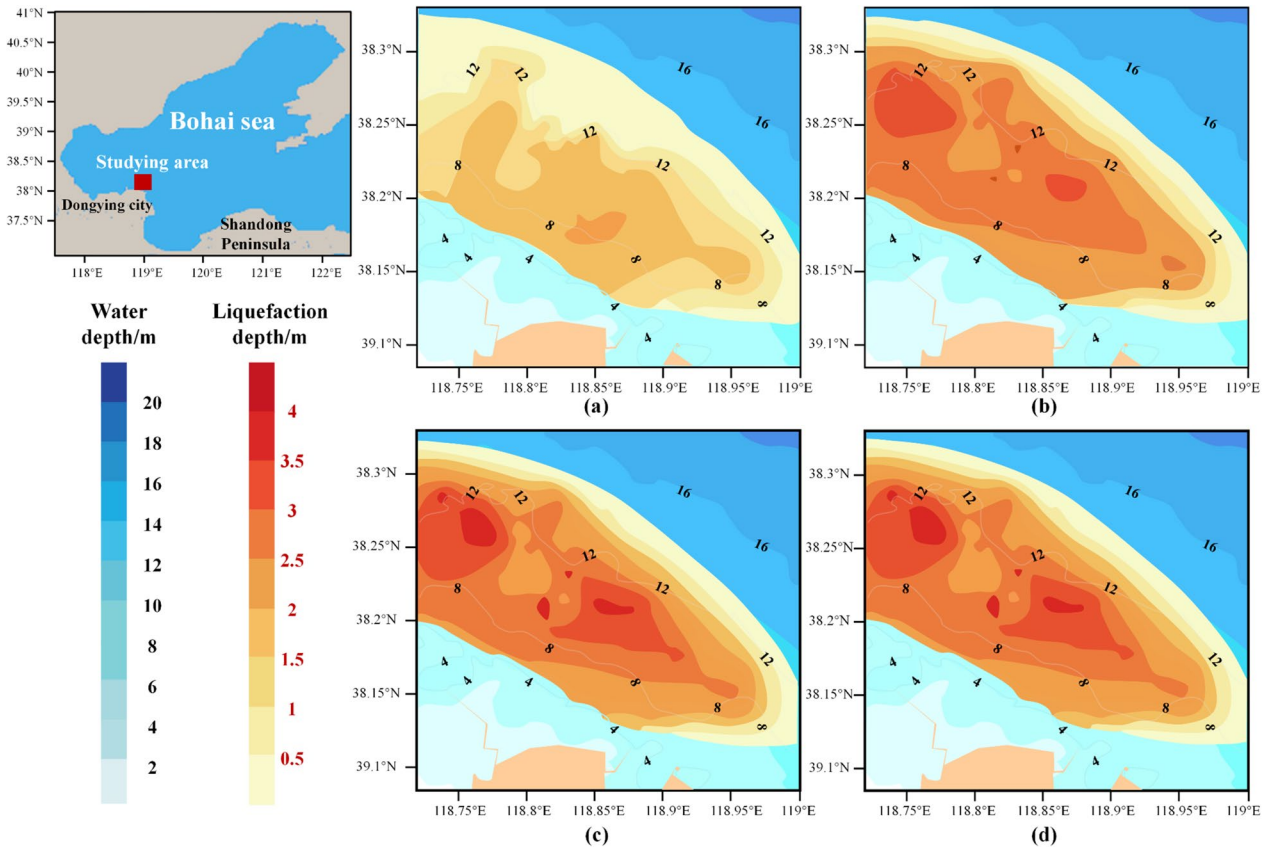

Fig. 13 Potential liquefaction depth of the seabed in different wave recurrence intervals: **a** wave recurrence period is 2 a; **b** wave recurrence period is 10 a; **c** wave recurrence period is 25 a; (**d**) wave recurrence period is 100 a (modified from Du et al. 2020)

surface liquefiable depth and the maximum calculated liquefaction depth was defined as the potential maximum liquefaction depth of the site, and the maximum liquefaction depth assessment of sediment under different wave recurrence conditions was mapped by the spatial interpolation method. Based on the above study, deterministic approaches are rarely used in the susceptibility of seabed liquefaction because the local adaptation of this method and the high data requirement constrain its application to large-scale areas.

Statistical approach

Juang et al. (2000) established a liquefaction limit state function by the artificial neural network method. Based on this function, a mapping function between the factor of safety (FS) and liquefaction probability was formulated and laid the foundation for mapping the risk of liquefaction potential. Jeng et al. (2004) used a single artificial neural network for seabed liquefaction prediction, and in 2009, they applied the multiple artificial neural network method to predict liquefaction under complex conditions. This method used a network constructed between multiple databases for accurate prediction of the results and was more adaptable to the prediction of the shallow seabed. Jeng (2013) compared the evaluation results of the two different network models mentioned above. He concluded that the multiple artificial neural network model with a network constructed between multiple databases can be realized for environmentally complex conditions. Hence, it could achieve an accurate prediction of liquefaction depth in the region between 0 and 1 m, which was more suitable for the shallow seabed. Cha et al. (2009, 2011) applied the multi-artificial neural network (MANN) model to predict the maximum liquefaction depth. They compared the simulation results with those of the poroelastic model and found that the difference between the results of the deterministic model and the conventional numerical simulation can be controlled within 10%. In addition, they found that the single artificial

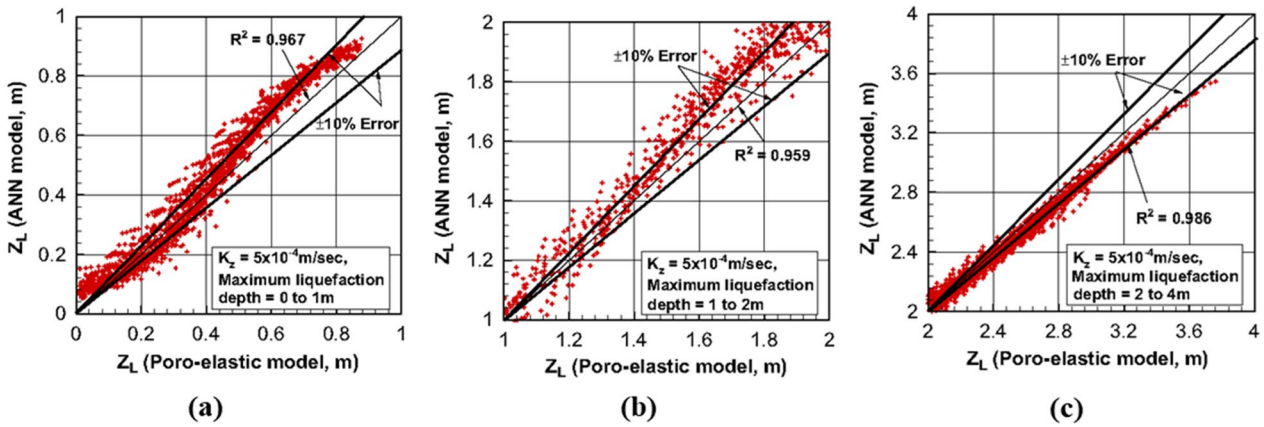

Fig. 14 Comparison of the wave-induced maximum liquefaction depths by the MANN model versus the poroelastic model, where $K_z = 10^{-4}$ m/s: **a** maximum liquefaction depth between 0 and 1 m, **b** maximum liquefaction depth between 1 and 3 m, and **c** maximum liquefaction depth between 3 and 5 m (modified from Cha et al. 2009; 2011)

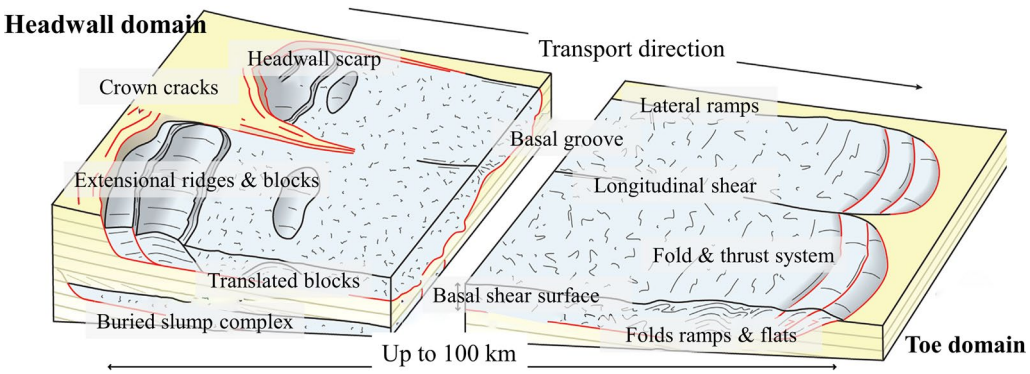

Fig. 15 Schematic illustration of the morphology and structures of a submarine landslide (modified from Scarselli 2020)

neural network model could predict the maximum liquefaction depth in the full range compared with the MANN model, and its accuracy was lower than that of the MANN model when predicting the extreme liquefaction depth (liquefaction depth less than 1 m or more than 3 m), as shown in Fig. 14. For the statistical approach, the susceptibility assessment is the result of extrapolation based on the statistics of historical events. Therefore, this method has poor relevance to the mechanisms of marine geological disasters.

Susceptibility of submarine landslides

Mechanism analysis of submarine landslides

Submarine landslides are an essential mechanism for the formation and movement of vast quantities of sediment on continental slopes. They occur when sediment is subjected to a downward force along a slope that exceeds its shear strength under the action of gravity or external loads (Urgeles et al. 2013). A schematic illustration is shown in Fig. 15. Headwall scarps, extensional ridges and blocks are the main structures that characterize the headwall domain. Headwall scarps are the boundaries between submarine landslides and undeformed, upslope strata (Scarselli 2020). Extensional features, such as blocks or elongated ridges separated by normal faults, are commonly observed close to headwall scarps. The downslope translation of collapsed material can lead to intense deformation, promoting the formation of several structural features, which include lateral margins, ramps and flats of the shear surface, basal grooves, longitudinal shear zones, folds and translated blocks (Scarselli 2020). Ramps are the steep segments of the basal shear surface that cut up or down through stratigraphy; flats are segments of the basal shear surface that are parallel to the bedding and interposed between ramps. Basal grooves or striations are linear to sinuous depressions in the basal shear surface (Bishop 1955; Zhu et al. 2015).

The triggering factors of submarine landslides are closely related to geological events (Canals et al. 2004). Earthquakes, submarine volcanic eruptions and gas hydrate disassociation may make the seabed unstable, as detailed in "Condition factors of susceptibility of submarine landslides" section. Sediment can be transformed on slopes with an inclination of 0.5–3°, moving distances up to hundreds of kilometers over time periods lasting less than an hour to several days, which is the biggest difference between submarine landslides and subaerial landslides (Hampton et al. 1996). Submarine landslides can seriously threaten the safety of submarine facilities, such as submarine pipelines and offshore platforms, and even cause tsunamis. The materials required for submarine landslides mainly come from continents (such as rivers) and continental shelves (mainly eroded and transported by ocean currents and storms) and include rocks, sediment, mud and mixtures of the three (Hance 2003; McAdoo et al. 2000; Guo et al. 2023a; Zhang et al. 2016). Submarine landslides occur on both active and passive margins, especially on continental slopes. Their evolution is similar to that of subaerial landslides and includes three stages: (1) the preinstability stage, in which the sediment or block is basically in a stable and complete state; (2) the instability stage, in which, for various reasons, a continuous shear zone or shear plane is formed in the block; (3) the stage after the failure stage, in which the slope slides until the movement basically stops; and (4) the restart stage, in which further slip of the block is related to the preexisting instability phenomenon. In the middle and late stages of submarine landslides, the debris flow gradually evolves, and the flow rate is relatively fast (Locat and Lee 2002; Li et al. 2012). When the failure state of the landslide evolves further, the sediment will evolve from a debris flow to a turbidity state. Since the unit density and shear strength of turbidite sediments are much lower than those of debris flows, the damage done to pipelines and subsea facilities by submarine landslides primarily occurs during the debris flow period (Guo et al. 2022a, 2023b).

Condition factors of susceptibility of submarine landslides

There is a close relationship between the condition factors of submarine landslides and the characteristics of the environment. Generally, the condition factors can be divided into loading conditions and seabed conditions.

Loading conditions

The condition factors of submarine landslides include oversteepening, seismic loading, storm-wave loading, rapid accumulation and underconsolidation, gas charging, gas hydrate disassociation, low tide, seepage, glacial loading, and volcanic island growth (Locat and Lee 2002; Hance 2003; Wang et al. 2020a; Nian et al. 2022; Guo et al. 2022d; Uri et al. 2009), as shown in Fig. 16. By

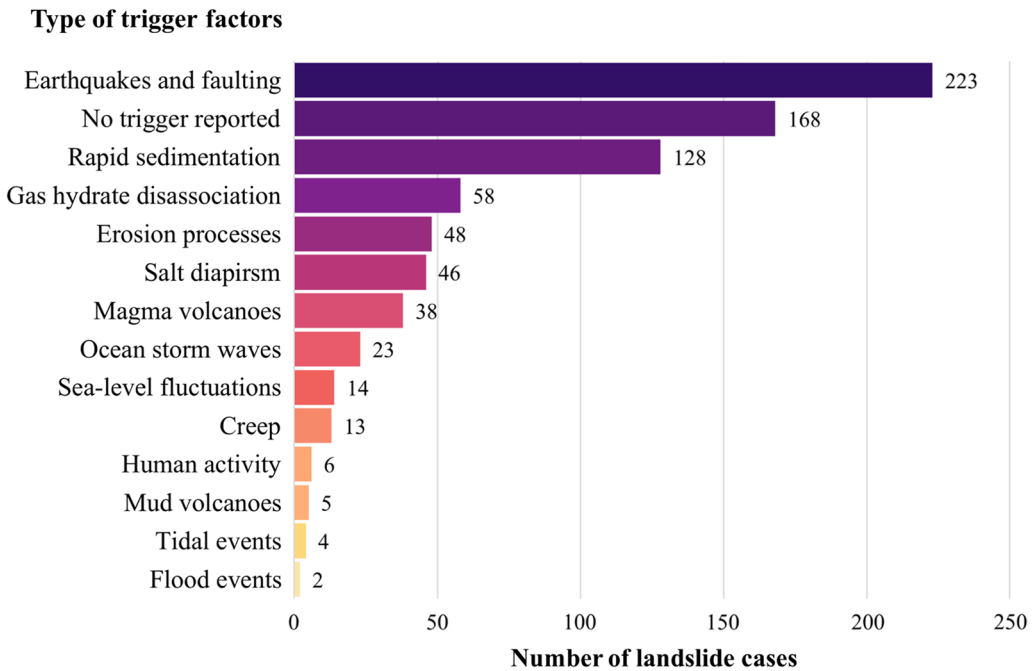

Fig. 16 Number of landslide cases associated with different trigger factors (modified by Zhu et al. 2018)

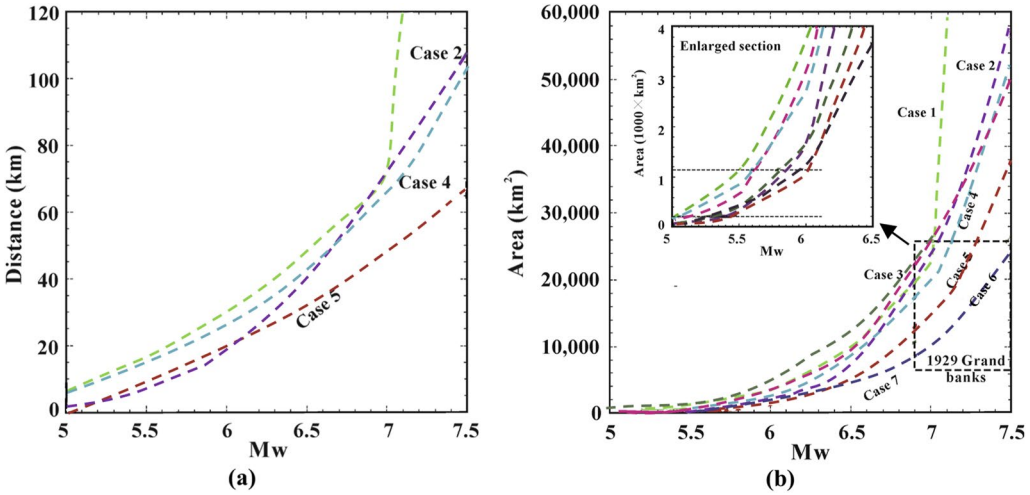

Fig. 17 The correlation between the earthquake magnitude and the scale of submarine landslides: **a** the correlation between the earthquake magnitude and the maximum distance to slope failure from fault rupture; **b** the correlation between the earthquake magnitude and the maximum area of slope failure (modified from Uri et al. 2009)

summarizing 534 submarine landslides, Zhu et al. (2018) found that the main trigger factors include (1) earthquakes and faults; (2) gas hydrate disassociation; and (3) rapid sedimentation. The percentage of submarine landslides caused by earthquakes exceeds 40%. These geological activities, as the triggering factors of submarine landslides, destabilize the slope by reducing the stability of the sediment structure (Zhang et al. 2018). These three triggers are discussed below.

Earthquakes are the most common trigger factor for submarine landslides. The oscillatory loading generated by an earthquake can produce elevated pore pressures in poorly drained sediments that lead to failure (Biscontin et al. 2006). In addition, oscillatory loading can affect sediment permeability, making it difficult to dissipate sediment pore water pressure and destabilizing the sediment for a long time (Camerlenghi et al. 2007). Earthquake intensity affects the location, distribution, and scale of submarine landslides in marine areas (Cornell 1968). In the study of submarine landslides on the continental slope of the U.S. Atlantic margin, Uri et al. (2009) summarized the relationship between earthquake magnitude and the scale of submarine landslides. They found that the greater the magnitude is, the greater the maximum distance and area of submarine landslides, as shown in Fig. 17. Earthquakes of smaller magnitude at a distance, however, can also trigger submarine landslides. Fan et al. (2020) investigated 85 submarine landslides in the Gulf of Mexico and found that 75 were triggered by surface wave dynamics from long-range earthquakes with magnitudes as low as 5. Uri et al. (2009) also studied the correlation between earthquake magnitude and maximum slope damage area and found a positive correlation between magnitude and maximum slope damaged area. In susceptibility studies, the effect of earthquakes on submarine landslide triggering has been measured by peak ground acceleration (PGA) values. PGA can be used to describe seismic motion attenuation relationships with the empirical correlation between the maximum ground acceleration observed at a site during a seismic event and the magnitude of the earthquake. Others have used probabilistic seismic hazard analysis (PSHA) to characterize the stochastic nature of earthquakes, which describes the relationship between ground shaking parameters (e.g., peak ground velocity, peak ground acceleration) and the mean echo period (Biscontin et al. 2004). This method also considers potential earthquake sources and seismic activity levels (Collico et al. 2020; Meunier et al. 2007).

Gas hydrates is solid, crystalline, ice-like substances consisting of water, methane, and small amounts of other gases that are commonly found where natural gas supplies are plentiful and temperature and pressure conditions are stable (Sultan et al. 2004a; Pietruszczak et al. 1996). The decomposition of natural gas hydrates is an important factor in triggering submarine landslides. Gas in marine sediments (usually methane) can form gas hydrates on the seafloor at moderate pressures, low temperatures, and sufficient gas concentrations. Changes in the temperature of the bottom water, the pore pressure of the sediment, the chemical properties of the gas and the salinity of the pore water can all reduce the stability of hydrates and promote the decomposition of the hydrates to gas (Chen et al. 2020; Song et al. 2019). The presence of these gases in sediment pore water will

cause an increase in pore water pressure, changing the strength of the sediment and reducing the compaction of the sediment. In this way, the strength of the sediment is substantially weakened, potentially forming a large area of submarine landslides (Liu et al. 2017b; Sultan et al. 2004b). One of the world's largest submarine landslides, the Storegga landslide off the coast of Norway, is considered likely to have been triggered by a process involving the breakdown of gas hydrates approximately 8000 years ago (Talling et al. 2014). Sultan (2007) assessed the impact of gas hydrate decomposition and dissolution on seabed stability due to sea level and temperature changes since the last ice age and theoretically calculated that the top of the gas hydrate-enriched zone was more prone to decomposition than the bottom.

Rapid sedimentation is another trigger factor of submarine landslides. This phenomenon dramatically alters sediment thickness, seafloor slope, and sediment distribution. The rapid deposition of sediments causes excess pore water pressure, which reduces the vertical effective stress and sediment strength and causes instability of the submarine slope (Chang et al. 2021). Sultan et al. (2004b) tested three different settling rates of 0.1, 0.2 and 0.4 m/ky, and the results showed that the greater the sedimentation rate, the greater the value of excess pore water pressure and the worse the sediment stability. In low-slope areas, rapid deposition reduces the surface roughness of the sediment, allowing sediment to be carried over long distances (Hance 2003). Fjords, estuarine deltas, submarine canyons and mid-ocean ridges are the main areas of sediment accumulation. A causal relationship can be found between the location of rapid sedimentation-induced submarine landslides and the location of estuarine deltas with high sedimentation rates worldwide.

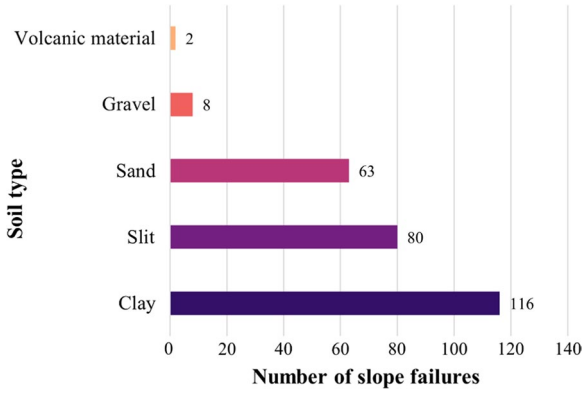

Fig. 18 Number of slope failures associated with different sediment types (modified from Hance 2003)

Substrate conditions

The physical and mechanical properties of the sediments (Guo et al. 2022b, 2022c, 2023c) have a great influence on the susceptibility of submarine landslides. The pore ratio and water content of marine sediments are multiple times higher than those of continental sediments, making marine sediments have low shear strengths, large liquid and plastic limits, and a high sensitivity to external loads. The particle composition of sediment is the main factor affecting the physical and mechanical properties of the sediment. In turn, the particle composition of the sediment is the main factor affecting its physical and mechanical properties (Owen 1987). The composition of the sediment in which submarine landslides occur is mainly clay, silt, sand, gravel and volcanic material, and its distribution depends on rivers and transport by currents and storms, as shown in Fig. 18. Hance (2003) summarized the particle composition of 266 submarine landslides and found that most of the landslides (> 65%) had more than one type of sediment particle, among which fine particles, i.e., clay and silt, were predominant. Because the pore water pressure in fine-grained sediments easily rises and is difficult to dissipate, such sediments are prone to instability and submarine landslides (Zhang et al. 2019b). The probability of submarine landslides in gravelly sediment is significantly lower than that in other sediment types because it is difficult for ocean currents to transport gravel longer distances offshore. In addition, compared with other cohesionless sediments, gravelly sediments have difficulty forming excessive pore water pressure (Hühnerbach et al. 2004).

Weak intercalated layers are regarded as one of the key factors in submarine landslides, and they play a pivotal role in determining the location and geometry of submarine landslide initiation. They are mostly found in contouritic clay deposits that formed along the glacial front during interglacial periods and are buried by glacial-marine sediments. It has been shown that the difference in strength and stiffness between weakly intercalated layers and adjacent layers can sometimes be up to 50% due to the formation of sediments in different depositional environments (Liu et al. 2017c).

Despite the physical and mechanical properties of the sediments, the geometry of the slope is also a condition factor for the occurrence of submarine landslides. The factors that reflect the slope geometry include slope angle, slope height, and slope length (Wang et al. 2018). Among them, the slope angle has the highest contribution to the occurrence of submarine landslides. Innocenti et al. (2020) used the maximum entropy model to screen and weight condition factors and found that the contribution of the slope factor was 82%. The influence of the slope angle on the stability of the submarine slope

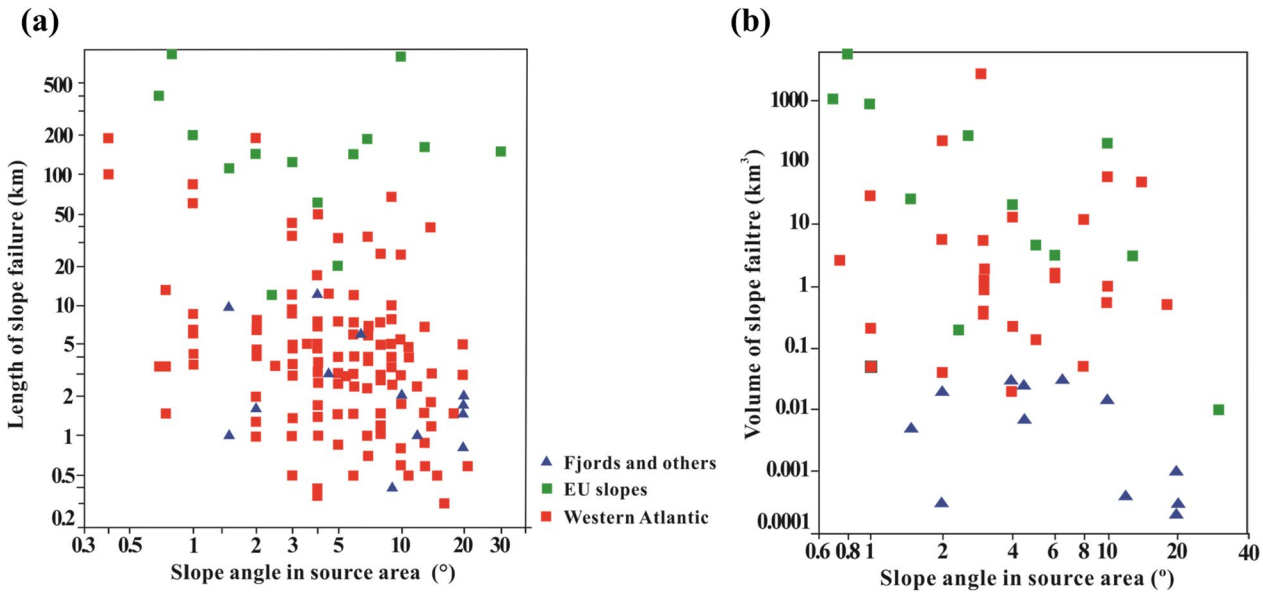

Fig. 19 Logarithmic scatter plot of slope instability parameters at different slope angles (modified from Hühnerbach and Masson 2004)

is reflected in the following two aspects: (1) the component of gravity down the slope rapidly increases so that the frictional force is unable to counteract the gravity component and (2) for a given slope length, an increase in the slope angle means an increasing height difference between the top and toe of the slope. As a result, the crustal stress on the toe of the slope along the horizontal direction increases significantly. Studying the characteristics of submarine landslides in the eastern and western North Atlantic, Hühnerbach et al. (2004) found that the slopes situated between 30 N and 45° N were mostly less than 5°, slopes with slope angles greater than 38° did not slide, and the largest and farthest traveling landslides tended to occur on low-angle slopes, as shown in Fig. 19. Zhang et al. (2012) found that under drained conditions, submarine slopes below 20° were in a stable state under static conditions. They also found that under undrained conditions caused by rapid accumulation and low permeability strata, the slopes would become unstable when the slope angle increased above 14°. The causes of slope steepening include faults, folding, and diapirism, which cause slope instability.

Advances in the susceptibility of submarine landslides

Recently, the susceptibility of submarine landslides has focused on the continental margin. Due to the possibility of triggering factors, most researchers have focused on earthquake-induced submarine landslides. The susceptibility of submarine landslides is evaluated either by analyzing the condition factor of its occurrence or by the state before its occurrence, i.e., the stability of submarine landslides. Among all susceptibility methods, the heuristic approach, deterministic approach and statistical approach are the most frequently used in determining the susceptibility of submarine landslides.

Heuristic approach

The AHP was applied by Li et al. (2014) to determine the weight of the factors responsible for the instability in the Baiyun Sag. Combined with the historical geological events and geological characteristics of the region, the evaluation index system of submarine slope instability was constructed with five indicators: U1 is the seafloor gradient; U2 is the sedimentation rate; U3 is the sea-level change; U4 is seismic forces; and U5 is the gas hydrate dissociation. The weight vector of evaluation indicators affecting submarine slope stability, evaluated by the comparison matrix, is written as A = (0.377, 0.204, 0.118, 0.193 and 0.108). The importance ranking for the evaluation indicator is seafloor gradient > sedimentation rate > sea-level change > seismic forces > gas hydrate dissociation, as shown in Table 5. The consistency ratio is 0.006, which indicates that the weighted coefficient is reasonable and efficient. As a traditional method, the heuristic approach can yield a qualitative assessment of the susceptibility of marine geological disasters. However, the high data requirement has restricted the development of the method.

Deterministic approach

The deterministic method, as the traditional method in submarine landslide susceptibility, can be used to

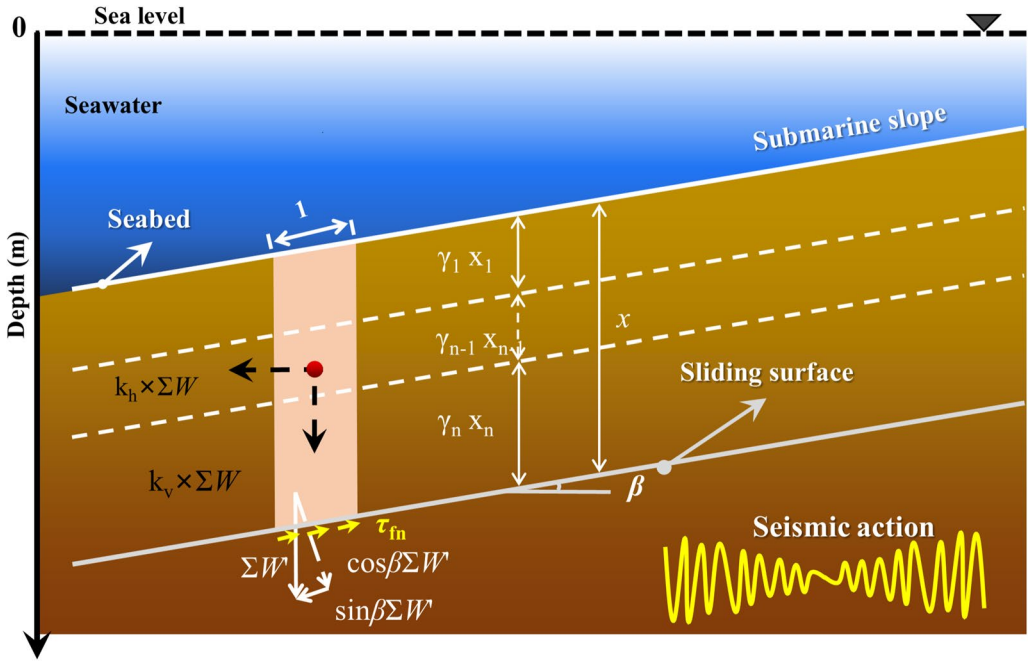

Fig. 20 Stress analysis of a submarine slope under seismic loading (modified from Nian et al. 2019)

analyze the stability of slopes, which is mostly quantified by using the factor of safety. The limit equilibrium method is mostly used to achieve quantitative analysis of submarine slope stability. Assuming the existence of a certain sliding surface, a submarine landslide occurs when the sliding force of a block on the sliding surface is greater than the shear strength (Nian et al. 2019). This process can be expressed as a factor of safety (FS); that is, when $FS > 1$, the slope is stable, and when $FS < 1$, a landslide will occur. Generally, external load factors and geological features are considered when establishing the factor of safety.

Nian et al. (2019) simplified a submarine slope as a rigid body and subjected it to four combinations of forces under quasistatic bidirectional seismic action. They analyzed the slope stability under bidirectional seismic loading in different slope directions, and the FS of the multilayer slope was established according to different force cases. The weakening effect of seabed sediment strength under seismic loading was also considered in the FS, as shown in Fig. 20. Based on GIS data processing and analysis, a digital elevation model (DEM) was established, and submarine topographic data were collected and analyzed. At the same time, the inverse distance weighting method was applied to realize the susceptibility mapping of submarine landslides from discrete points to the whole area of the subaerial slope in the northeastern South China Sea (SCS), as shown in Fig. 21. The accuracy of this method depends primarily on the physical and mechanical data of the marine sediment layers. In addition, it relies on the calculation model for the submarine slope stability and the selection of interpolation methods and interpolation points.

Wang et al. (2021) analyzed submarine geomorphology, seismic loading and seabed characteristics to evaluate the stability of submarine landslides in the northeastern region of the SCS. They established a DEM for the study area and derived large-scale PGA maps under different exceedance probabilities (EPs) by the Chinese probability seismic hazard analysis (CPSHA) method. In addition, three-dimensional continuous models for seafloor sediment properties were obtained using a proposed best-fit distribution-based kriging method. Based on a related study by Nian et al. (2019), they further employed an infinite slope model based on the limit equilibrium method to quantify the stability of submarine slopes at a larger scale using the above data and generated seafloor stability FS maps for the SCS research area under earthquakes of different exceedance probabilities, as shown in Fig. 22. For example, "63% in 50 years" means that the exceedance probability under seismic hazards in this study area is 63% in 50 years. The exceedance probability refers to the probability that a certain value will be exceeded in a predefined future time period (Wang et al. 2021). For the large research area in this study, the current pool of seafloor sediment property data is still very limited, which restricts the accuracy of the assessment results. The infinite slope model and quasistatic analysis method may

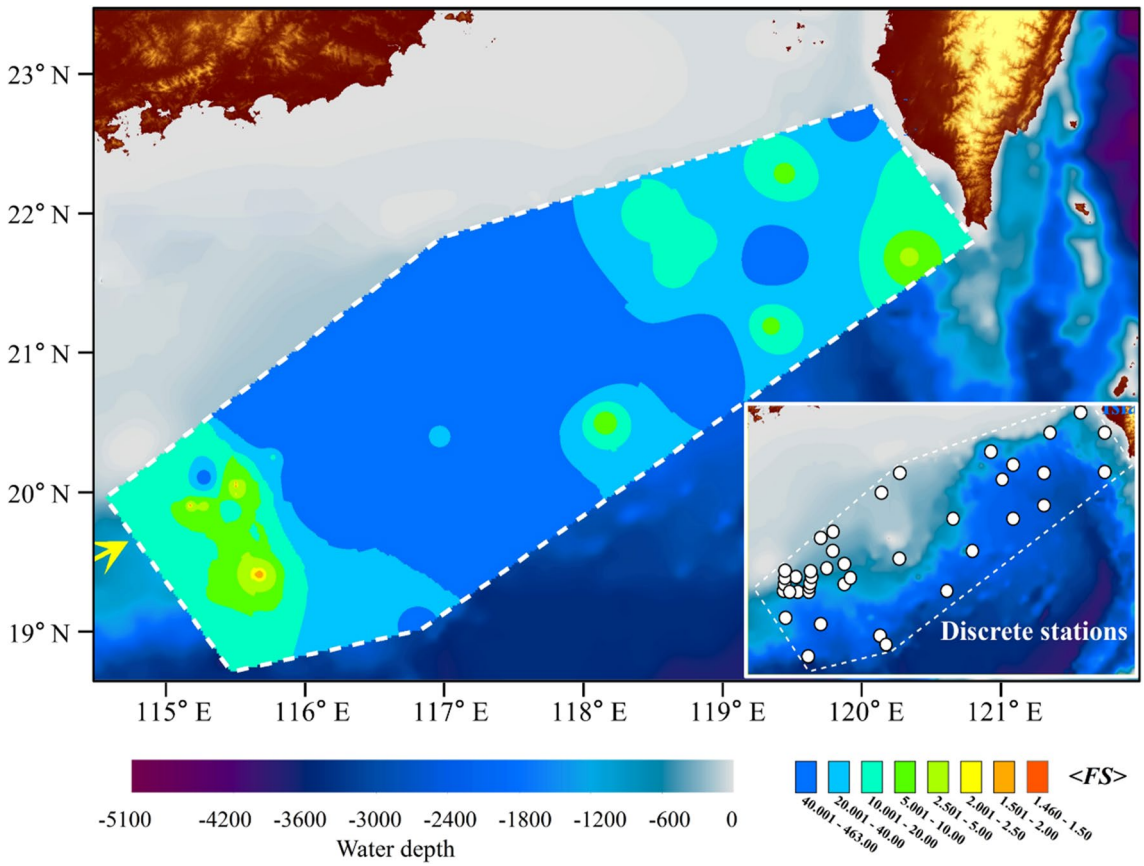

Fig. 21 Susceptibility map of submarine landslides on the northeast continental slope of the SCS. The map of known stations of physical and mechanical parameters and seismic distribution of marine sediment distributed on the continental slope of the northern SCS is shown in the lower right corner (modified from Nian et al. 2019)

oversimplify the dynamic nature of seismic-induced submarine landslides, and more high-fidelity analysis may be considered with the accumulation of more data in the region.

Statistical approach

Borrell et al. (2016) used the Wi-index bivariate method to calculate the weights of different categories of factors, such as landslide location, earthquake density of the study area, seafloor slope angle, seafloor composition, and the area of active faults, and generated a submarine landslide susceptibility map of the Spanish continental margin using GIS, as shown in Fig. 23. Wi index values can indicate the close relationship between the seabed sediment classes and landslide occurrence. Submarine landslides were more frequent on continental slopes with slope angles between 0.8 and 4%, but the maximum values of the slope angle were not associated with the highest density of landslides. This method has strong operability, but it is clear there is a need to gather more data and extend the study area to obtain a more conclusive statistical analysis.

Lapa et al. (2020) focused on the effects of water depth, mean slope, seabed curvature, and sediment properties on the stability of the Aveiro Canyon Head (Portugal) submarine slope, and the bivariate information value method and logistic regression method were used to generate susceptibility maps of the area to compare the accuracy of the two methods, as shown in Fig. 24. The validation of the receiver operating characteristic curves (ROCs) for the evaluation results showed that the logistic regression model (AUC = 0.8296) was more consistent than the bivariate information value method (AUC = 0.7908).

Innocenti et al. (2020) mapped the susceptibility of submarine landslides in European seas using the maximum entropy model (MaxEnt) and landslide cartography acquired from European Marine Observation and Data Network (EMODnet) Geology. Thirty-three condition factors were carried out using the r.param.scale module of the GRASS open-source GIS software, where

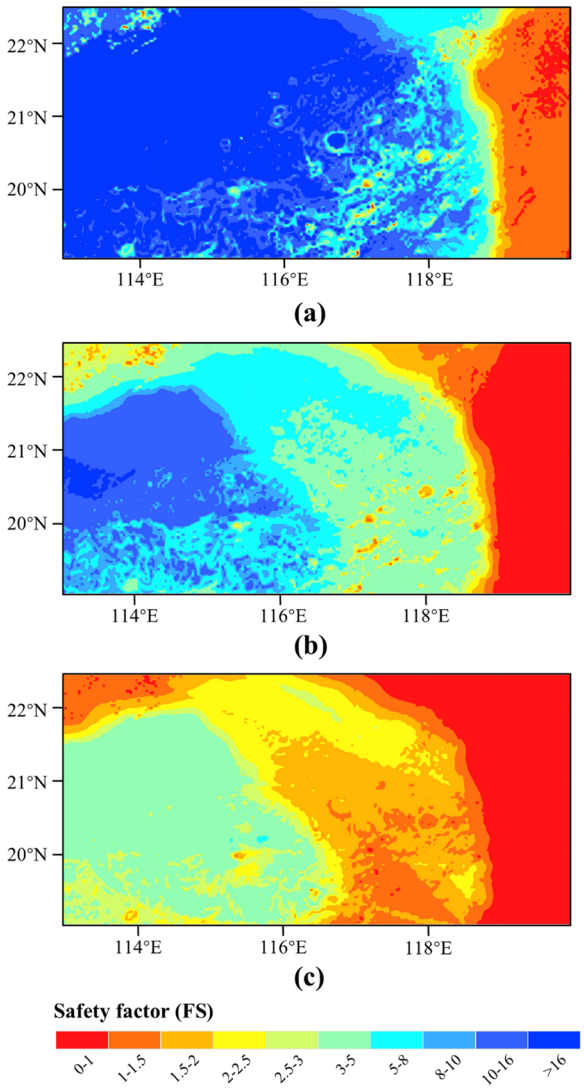

Fig. 22 FS of seabed stability in the SCS under different earthquake exceedance probabilities: **a** 63% in 50 years; **b** 10% in 50 years; **c** 2% in 50 years (modified from Wang et al. 2021)

the slope and bathymetry factors were retained through filtering by MaxEnt. Linear elements and polygonal elements were transformed into point elements for MaxEnt, and individual data with errors were excluded. Of these, 85% (2064 points) were used for model training, and 15% (364 points) were used for testing, resulting in a submarine landslide susceptibility map, as shown in Fig. 25. The diverse data types and rich data volume provide the historical information basis for the susceptibility assessment. Thus, we note that the evaluation results are closer to the actual situation and have certain reference value for engineering construction.

Future challenges

The susceptibility analysis of marine geological disasters is undergoing a transition from qualitative analysis to quantitative analysis and from sampling analysis to a combination of deterministic and nondeterministic analysis. The evaluation results are more accurate, specific, and applicable. Despite numerous promising results, this field is still in the immature stage, and many challenges and technical bottlenecks need to be addressed. These issues can be divided into four main aspects: the integrality of the susceptibility system, the comprehensiveness of the disaster inventory, the accuracy of the condition factors, and the precision of the assessment model.

(1) The susceptibility system of marine geological disasters needs to be improved. Currently, the susceptibility system of terrestrial geohazards is still being used as a reference. The existing susceptibility system and corresponding methods are not specifically formulated for the characteristics of marine geological disasters, resulting in the lack of application of susceptibility maps. Relevant academic organizations are encouraged to implement the marine geological disaster susceptibility system to promote the development of this field.

(2) The disaster inventory of marine geological disasters is not comprehensive, and the amount of data is insufficient to understand the susceptibility of large-scale areas. The characteristics of marine geological disasters (i.e., easy occurrence, wide distribution, and difficult observation) make it difficult for researchers to obtain real-time data to build information inventories. Therefore, long-term in situ observational studies should be supported to obtain more valuable data and build an information-sharing platform to facilitate researchers' collection of data on marine geological disasters.

(3) The process of marine geological disasters is very complex, and their mechanisms are still unclear. The formation of each disaster is affected by many factors, e.g., seabed and loading conditions. Significantly, marine geological disasters easily develop into disaster chains, which brings serious challenges to susceptibility assessment, and thus, it is difficult to select condition factors for susceptibility assessment. We suggest that studies on the triggering mechanisms of marine geological disasters should be strengthened to reproduce their origins and development processes, involving but not limited to physical model experiments, high-precision numerical simulations, and large-scale long-term observations.

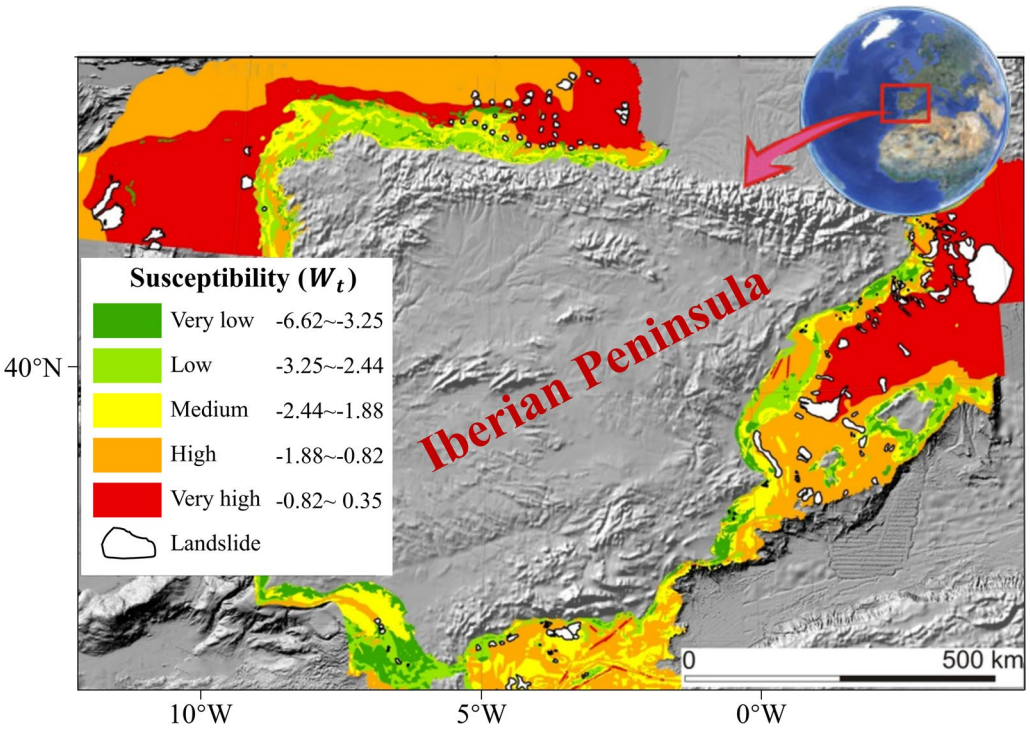

Fig. 23 Susceptibility map of the Spanish continental margin (modified from Borrell et al. 2016)

(4) The predictive performances of the susceptibility models remain a difficult and uncertain task at different scales. All methods have limitations in susceptibility, increasing the gap between the estimated results and the actual situation. To improve the accuracy of susceptibility results, more appropriate susceptibility methods should be selected according to the geological and topographical location of the study area. In addition, we recommend concentrating on the development of more reliable methods involving multisource data to increase the credibility and usefulness of the data on the susceptibility of marine geological disasters.

Conclusions

Since early attempts in the 2000s to ascertain susceptibility results for marine geological disasters, many studies have been published demonstrating achievements in assessing marine geological disaster susceptibility. In this review, we focused on the susceptibility of two typical marine geological disasters (i.e., seabed liquefaction and submarine landslides) and systematically summarized the development history, methods, results, problems, and future directions. The conclusions are as follows.

(1) Based on a literature review using the extensive literature database, we summarized the susceptibility methods. The most common methods for susceptibility were the heuristic approach, the deterministic approach, and the statistical approach. Although some methods performed better than others, no single method proved to be superior in all conditions. Evidently, the selection of susceptibility methods should focus on the geological and topographical settings of the study area. Traditional methods, such as AHP, were widely applied in the early stages. However, in recent years, data processing methods such as random forest, neural network, machine learning, and support vector machine have developed rapidly, replacing traditional mathematical and statistical methods, and will become the mainstream means of susceptibility assessment in the future, as shown in Fig. 3.

(2) The susceptibility of two typical geological disasters, i.e., seabed liquefaction and submarine landslides, is reviewed in detail. The accuracy of the assessment results depends on the comprehension of trigger mechanisms and the selection of condition factors of the disaster. In addition, most studies currently focus on relatively small areas of intensive marine engineering and human activities; clearly, more studies of large-scale areas and large regions are necessary.

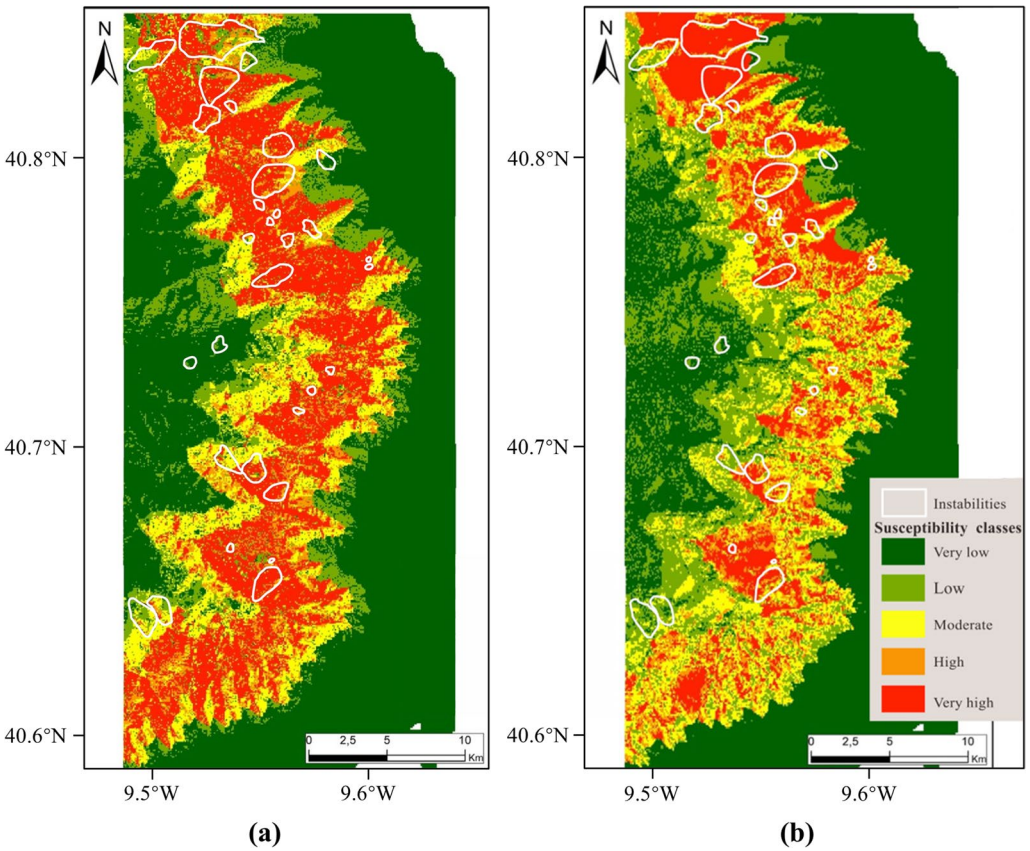

Fig. 24 Susceptibility maps with all factors based on different models: **a** information value (IV) model; **b** logistic regression (LR) model. White polygons correspond to the delimitations of the identified instabilities (modified from Lapa et al. 2020)

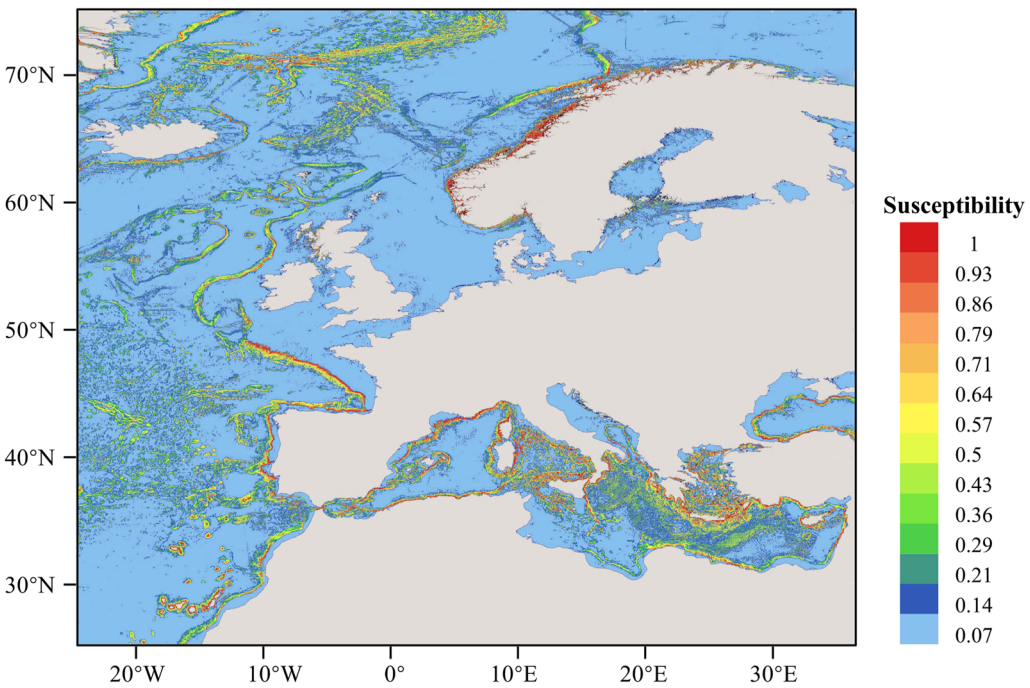

Fig. 25 Submarine landslide susceptibility map in the European Sea area. A higher susceptibility value indicates that the area is more prone to submarine landslides (modified from Innocenti et al. 2020)

(3) There are four main difficulties in the study of the susceptibility of marine geological disasters, involving the integrality of the susceptibility system, the comprehensiveness of the disaster inventory, the accuracy of the condition factors, and the precision of the assessment model. In response to the above problems, we suggest that relevant organizations should focus on the construction of the susceptibility system and the study of the triggering mechanisms of marine geological disasters. Long-term in situ observations should also be supported to obtain more data for improving the disaster inventory. Ultimately, more reliable methods can help improve the credibility and usefulness of susceptibility mapping of marine geological disasters.

Abbreviations

AHP	Analytic hierarchy process
AUC	Area under the curve (ROC value)
CI	Consistency index
CPSHA	Chinese Probability Seismic Hazard Analysis
CR	Consistency ratio
CRR	Cyclic resist resistance ratio
CSR	Cyclic stress ratio
DEM	Digital elevation model
EMODnet	European Marine Observation and Data Network
Eps	Exceedance probabilities
FS	Safety factor
GIS	Geographic Information System
IAEG	International Association for Engineering Geology and the Environment
IDW	Inverse distance weighting
ISRM	International Society for Rock Mechanics
ISSMGE	International Society for Soil Mechanics and Geotechnical Engineering
JTC-1	Joint Technical Committee on Landslides and Engineered Slopes
LR	Logistic regression
m/ky	Meter per 1000 years
MANN	Multiartificial Neural Network
MaxEnt	Maximum Entropy Model
NSW	Nearshore spectral windwave
PGA	Peak ground acceleration
PSHA	Probabilistic seismic hazard analysis
ROC	Receiver operating characteristic
SCS	South China Sea

Acknowledgements
The authors thank all the scholars in the references for their contributions in their research fields. In addition, the authors would like to thank Han Gao, Shuyu Zhang, Xiaotian Xie, and Yujun Tian for their contributions in the design and production of the figures.

Author contributions
XL contributed to the conception, design and drafting of the work. YW contributed to the acquisition, analysis, interpretation of data, and drafting of the work. H contributed to the drafting of the work. SG contributed to the conception, design and drafting of the work. All authors read and approved the final manuscript.

Funding
Funding for the research has been supported by the National Natural Science Foundation of China (42022052 and 42277138) and the Shandong Provincial Natural Science Foundation (ZR2020YQ29).

Availability of data and materials
All data, models, and code generated or used during the study appear in the submitted article.

Declarations

Competing interests
The authors declare that they have no competing interests.

Author details
[1]Shandong Provincial Key Laboratory of Marine Environment and Geological Engineering, Ocean University of China, Qingdao 266100, China. [2]Department of Civil, Environmental, and Geomatic Engineering, University College London, London WC1E 6BT, UK. [3]College of Engineering, Ocean University of China, Qingdao 266100, China. [4]Laboratory for Marine Geology, Qingdao National Laboratory for Marine Science and Technology, Qingdao 266061, China.

Received: 19 December 2022 Accepted: 4 March 2023
Published online: 27 March 2023

References

Aleotti P, Chowdhury R (1999) Landslide hazard assessment: summary review and new perspectives. Bull Eng Geol Env 58(1):21–44. https://doi.org/10.1007/s100640050066

Al-Umar M, Fall M, Daneshfar B (2020) GIS-based modeling of snowmelt-induced landslide susceptibility of sensitive marine clays. Geoenviron Disasters 7:9. https://doi.org/10.1186/s40677-020-0142-8

Avdievitch NN, Coe JA (2022) Submarine landslide susceptibility mapping in recently deglaciated terrain, Glacier Bay, Alaska. Front Earth Sci 10:821188. https://doi.org/10.3389/feart.2022.821188

Babak O, Deutsch CV (2009) Statistical approach to inverse distance interpolation. Stoch Env Res Risk Assess 23:543–553. https://doi.org/10.1007/s00477-008-0226-6

Bian C, Liu X, Zhou Z, Chen Z, Wang T, Gu Y (2020) Calculation of winds induced bottom wave orbital velocity using the empirical mode decomposition method. J Atmos Oceanic Tech 37(5):889–900. https://doi.org/10.1175/JTECH-D-19-0185.1

Biscontin G, Pestana JM (2006) Factors affecting seismic response of submarine slopes. Nat Hazard 6:97–107. https://doi.org/10.5194/nhess-6-97-2006

Biscontin G, Pestana JM, Nadim F (2004) Seismic triggering of submarine slides in soft cohesive soil deposits. Mar Geol 203(3–4):341–354. https://doi.org/10.1016/S0025-3227(03)00314-1

Bishop AW (1955) The use of the slip circle in the stability analysis of slopes. Geotechnique 5(1):7–17. https://doi.org/10.1680/geot.1955.5.1.7

Bjerrum J (1973) Geotechnical problem involved in foundations of structures in the North Sea. Géotechnique 23(3):319–358. https://doi.org/10.1680/geot.1973.23.3.319

Bokati L, Velasco A, Kreinovich V (2022) Scale-invariance and fuzzy techniques explain the empirical success of inverse distance weighting and of dual inverse distance weighting in geosciences. In: Bede B, Ceberio M (eds) Fuzzy information processing 2020. Advances in intelligent systems and computing, vol 1337. Springer, Cham, pp 379–390

Borrell M, Somoza L, León R, Medialdea T, Gonzalez FJ, Gimenez-Moreno CJ (2016) GIS catalogue of submarine landslides in the Spanish Continental Shelf: Potential and difficulties for susceptibility assessment. In: Lamarche G (ed) Submarine mass movements and their consequences. Advances in natural and technological hazards research, vol 41. Springer, Cham, pp 499–508

Bucci MG, Tuttleb MP (2022) 2.20 - Liquefaction susceptibility and hazard mapping: insights from case histories of earthquake-induced liquefaction. Treatise Geomorphol 2:563–582. https://doi.org/10.1016/B978-0-12-818234-5.00054-7

Bucci MG, Micallef A, Urlaub M, Mountjoy J, Barrettd R (2022) A global review of subaqueous spreading and its morphological and sedimentological characteristics: a database for highlighting the current state of the art. Geomorphology 414:108397. https://doi.org/10.1016/j.geomorph.2022.108397

Budetta P, Santo A, Vivenzio F (2008) Landslide hazard mapping along the coastline of the Cilento region (Italy) by means of a GIS-based parameter rating approach. Geomorphology 94(3–4):340–352. https://doi.org/10.1016/j.geomorph.2006.10.034

Camargo JMR, Silva MVB, Ferreira Júnior AV, Araújo TCM (2019) Marine geohazards: a bibliometric-based review. Geosciences 9(2):100. https://doi.org/10.3390/geosciences9020100

Camerlenghi A, Urgeles R, Ercilla G, Brückmann W (2007) Scientific ocean drilling behind the assessment of geo-hazards from submarine slides. Sci Drill 4:45–47. https://doi.org/10.2204/iodp.sd.4.14.2007

Can T, Nefeslioglu HA, Gokceoglu C, Sonmez H, Duman TY (2005) Susceptibility assessments of shallow earthflows triggered by heavy rainfall at three catchments by logistic regression analyses. Geomorphology 72(1–4):250–271. https://doi.org/10.1016/j.geomorph.2005.05.011

Canals M, Lastras G, Urgeles R, Casamor JL, Mienert J, Cattaneo A, Batist MD, Haflidason H, Imbo Y, Laberg JS, Locat J, Long D, Longva O, Masson DG, Sultan N, Trincardi F, Bryn P (2004) Slope failure dynamics and impacts from seafloor and shallow sub-seafloor geophysical data: case studies from the COSTA project. Mar Geol 213(1–4):9–72. https://doi.org/10.1016/j.margeo.2004.10.001

Cao Z, Gu Q, Huang Z, Fu J (2022) Risk assessment of fault water inrush during deep mining. Int J Min Sci Technol 32(2):423–434. https://doi.org/10.1016/j.ijmst.2022.01.005

Cha DF, Zhang H, Blumenstein M, Jeng DS (2009) Accurate prediction of wave-induced seabed liquefaction at shallow depths using multi-artificial neural networks. J Coast Res Spec Issue 56:927–931

Cha DF, Zhang H, Blumenstein M (2011) Prediction of maximum wave-induced liquefaction in porous seabed using multi-artificial neural network model. Ocean Eng 38(7):878–887. https://doi.org/10.1016/j.oceaneng.2010.08.002

Chang C, Chien L, Chang Y (2004) 3-D liquefaction potential analysis of seabed at nearshore area. J Mar Sci Technol 12(3):2. https://doi.org/10.51400/2709-6998.2232

Chang Y, Mitchell NC, Quartau R (2021) Landslides in the upper submarine slopes of volcanic islands: the Central Azores. Geochem Geophys Geosyst 22(10):e2021GC009833. https://doi.org/10.1029/2021GC009833

Chen Y, Zhang L, Liao C, Jiang M, Peng M (2020) A two-stage probabilistic approach for the risk assessment of submarine landslides induced by gas hydrate exploitation. Appl Ocean Res. https://doi.org/10.1016/j.apor.2020.102158

Chiocci FL, Cattaneo A, Urgeles R (2011) Seafloor mapping for geohazard assessment: state of the art. Mar Geophys Res 32:1–11. https://doi.org/10.1007/s11001-011-9139-8

Collico S, Arroyo M, Urgeles R, Gràcia E, Devincenzi M, Peréz N (2020) Probabilistic mapping of earthquake-induced submarine landslide susceptibility in the South-West Iberian margin. Mar Geol 429:106296. https://doi.org/10.1016/j.margeo.2020.106296

Cornell CA (1968) Engineering seismic risk analysis. Bull Seismol Soc Am 58(5):1583–1606. https://doi.org/10.1785/BSSA0580051583

Cuomo S (2020) Modelling of flowslides and debris avalanches in natural and engineered slopes: a review. Geoenviron Disasters 7:1. https://doi.org/10.1186/s40677-019-0133-9

Curtarelli M, Leão J, Ogashawara I, Lorenzzetti J, Stech J (2015) Assessment of spatial interpolation methods to map the bathymetry of an Amazonian Hydroelectric Reservoir to aid in decision making for water management. Int J Geo-Inf 4(1):220–235. https://doi.org/10.3390/ijgi4010220

Du X, Sun Y, Song Y, Xiu Z (2020) Wave-induced liquefaction hazard assessment and liquefaction depth distribution: a case study in the Yellow River Estuary, China. IOP Conf Ser Earth Environ Sci 569:012011. https://doi.org/10.1088/1755-1315/569/1/012011

Fan W, McGuire JJ, Shearer PM (2020) Abundant spontaneous and dynamically triggered submarine landslides in the Gulf of Mexico. Geophys Res Lett 47(12):e2020GL087213. https://doi.org/10.1029/2020GL087213

Felicísimo AM, Cuartero A, Remondo J, Quirós E (2013) Mapping landslide susceptibility with logistic regression, multiple adaptive regression splines, classification and regression trees, and maximum entropy methods: a comparative study. Landslides 10:175–189. https://doi.org/10.1007/s10346-012-0320-1

Fell R, Corominas J, Bonnard C, Cascini L, Leroi E, Savage WZ (2008) Guidelines for landslide susceptibility, hazard and risk zoning for land use planning. Eng Geol 102(3–4):85–98. https://doi.org/10.1016/j.enggeo.2008.03.022

Gamboa D, Omira R, Terrinha P (2021) A database of submarine landslides offshore West and Southwest Iberia. Sci Data 8:185. https://doi.org/10.1038/s41597-021-00969-w

Gatter R, Clare MA, Kuhlmann J, Huhn K (2021) Characterisation of weak layers, physical controls on their global distribution and their role in submarine landslide formation. Earth-Sci Rev 223:103845. https://doi.org/10.1016/j.earscirev.2021.103845

Guo X, Zheng D, Nian T, Lv L (2019) Large-scale seafloor stability evaluation of the northern continental slope of South China Sea. Mar Georesour Geotechnol 38(7):804–817. https://doi.org/10.1080/1064119X.2019.1632996

Guo X, Liu X, Hong Z, Li M, Luo Q (2022a) Evaluation of instantaneous impact forces on fixed pipelines from submarine slumps. Landslides 19:2889–2903. https://doi.org/10.1007/s10346-022-01950-3

Guo X, Stoesser T, Nian T, Jia Y, Liu X (2022b) Effect of pipeline surface roughness on peak impact forces caused by hydrodynamic submarine mudflow. Ocean Eng 243:110184. https://doi.org/10.1016/j.oceaneng.2021.110184

Guo X, Nian T, Wang D, Gu Z (2022c) Evaluation of undrained shear strength of surficial marine clays using ball penetration-based CFD modelling. Acta Geotech 17(5):1627–1643. https://doi.org/10.1007/s11440-021-01347-x

Guo X, Nian T, Zhao W, Gu Z, Liu C, Liu X, Jia Y (2022d) Centrifuge experiment on the penetration test for evaluating undrained strength of deep-sea surface soils. Int J Min Sci Technol 32(2):363–373. https://doi.org/10.1016/j.ijmst.2021.12.005

Guo X, Liu Z, Zheng J, Luo Q, Liu X (2023a) Bearing capacity factors of T-bar from surficial to stable penetration into deep-sea sediments. Soil Dyn Earthq Eng 165:107671. https://doi.org/10.1016/j.soildyn.2022.107671

Guo X, Nian T, Fu C, Zheng D (2023b) Numerical investigation of the landslide cover thickness effect on the drag forces acting on submarine pipelines. J Waterw Port Coast Ocean Eng 149(2):04022032. https://doi.org/10.1061/JWPED5/WWENG-1869

Guo X, Stoesser T, Zheng D, Luo Q, Liu X, Nian T (2023c) A methodology to predict the run-out distance of submarine landslides. Comput Geotech 153:105073. https://doi.org/10.1016/j.compgeo.2022.105073

Guzzetti F, Reichenbach P, Cardinali M, Galli M, Ardizzone F (2005) Probabilistic landslide hazard assessment at the basin scale. Geomorphology 72(1–4):272–299. https://doi.org/10.1016/j.geomorph.2005.06.002

Guzzetti F (2006) Landslide hazard and risk assessment. Dissertation, Universitäts-und Landesbibliothek Bonn

Hadi SJ, Tombul M (2018) Comparison of spatial interpolation methods of precipitation and temperature using multiple integration periods. J Indian Soc Remote Sens 46:1187–1199. https://doi.org/10.1007/s12524-018-0783-1

Hampton MA, Lee HJ, Locat J (1996) Submarine landslides. Rev Geophys 34(1):33–59. https://doi.org/10.1029/95RG03287

Hance JJ (2003) Submarine slope stability: development of a database and assessment of seafloor slope stability based on published literature. Dissertation, University of Texas at Austin

Hitchcock C, Givler R, Angell M, Hooper J (2010) GIS-based assessment of submarine mudflow hazard offshore of the Mississippi Delta, Gulf of Mexico. In: Mosher DC (ed) Submarine mass movements and their consequences. Advances in natural and technological hazards research, vol 28. Springer, Dordrecht, pp 353–364

Huang Y, Bao Y, Zhang M, Liu C, Lu P (2015) Analysis of the mechanism of seabed liquefaction induced by waves and related seabed protection. Nat Hazards 79:1399–1408. https://doi.org/10.1007/s11069-015-1897-1

Hühnerbach V, Masson DG (2004) Landslides in the North Atlantic and its adjacent seas: an analysis of their morphology, setting and

behaviour. Mar Geol 213(1–4):343–362. https://doi.org/10.1016/j.margeo.2004.10.013
Hutchinson MF (1993) On thin plate splines and kriging. In: Tarter ME (ed) Computing science and statistics, vol 25. University of California, Berkeley, pp 55–62
Ikari MJ, Strasser M, Saffer DM, Kopfa AJ (2011) Submarine landslide potential near the megasplay fault at the Nankai subduction zone. Earth Planet Sci Lett 312(3–4):453–462. https://doi.org/10.1016/j.epsl.2011.10.024
Innocenti C, Battaglini L, D'Angelo S, Fiorentino A (2020) Submarine landslides: mapping the susceptibility in European seas. Q J Eng Geol Hydrogeol 54(1):qjegh2020–qjegh2027. https://doi.org/10.1144/qjegh2020-027
Ishihara K (1993) Liquefaction and flow failure during earthquakes. Géotechnique 43(3):351–451. https://doi.org/10.1680/geot.1993.43.3.351
Ishinara K, Yamazaki A (1984) Analysis of wave-induced liquefaction in seabed deposits of sand. Soils Found 24(3):85–100. https://doi.org/10.3208/sandf1972.24.3_85
Jeng DS (1997) Wave-induced seabed instability in front of a breakwater. Ocean Eng 24(10):887–917. https://doi.org/10.1016/S0029-8018(96)00046-7
Jeng DS (2013) Porous models for wave-seabed interactions. Springer, Berlin
Jeng DS, Cha D, Blumenstein M (2004) Neural network model for the prediction of wave-induced liquefaction potential. Ocean Eng 31(17–18):2073–2086. https://doi.org/10.1016/j.oceaneng.2004.05.006
Jeng DS, Seymour B, Gao F, Wu Y (2007) Transient and cumulative response mechanisms of pore water pressure in seabed soils under wave loading. Sci China Press 37(1):91–98 (**in Chinese**)
Jia Y, Zhang L, Zheng J, Liu X, Jeng D, Shan H (2014) Effects of wave-induced seabed liquefaction on sediment re-suspension in the Yellow River Delta. Ocean Eng 89:146–156. https://doi.org/10.1016/j.oceaneng.2014.08.004
Jia Y, Zhu C, Liu L, Wang D (2016) Marine geohazards: review and future perspective. Acta Geol Sin-Engl Edition 90:1455–1470. https://doi.org/10.1111/1755-6724.12779
Juang CH, Chen CJ, Jiang T, Andrus RD (2000) Risk-based liquefaction potential evaluation using standard penetration tests. Can Geotech J 37(6):1195–1208. https://doi.org/10.1139/t00-064
Kleijnen JPC (2009) Kriging metamodeling in simulation: a review. Eur J Oper Res 192(3):707–716. https://doi.org/10.1016/j.ejor.2007.10.013
Lacasse S, Nadim F, Boylan N, Liu Z, Choi YJ (2019) Risk assessment and management for geotechnical design of offshore installations. Paper presented at the Offshore Technology Conference, Houston, Texas, May 2019
Lapa N, Marques FMFS, Rodrigues A (2020) Aveiro Canyon Head (Portugal) submarine slope instability assessment. Appl Sci 10(24):9038. https://doi.org/10.3390/app10249038
Lee S (2004) Application of likelihood ratio and logistic regression models to landslide susceptibility mapping using GIS. Environ Manag 34:223–232. https://doi.org/10.1007/s00267-003-0077-3
León R, Somoza L (2011) GIS-based mapping for marine geohazards in seabed fluid leakage areas (Gulf of Cadiz, Spain). Mar Geophys Res 32:207–222. https://doi.org/10.1007/s11001-011-9135-z
Li J, Xiu Z, Shen H, Jiang F (2012) A review of the studies on submarine mass movement. Coast Eng 31(04):67–78 (**in Chinese**)
Li C, Wu S, Zhu Z, Bao X (2014) The assessment of submarine slope instability in Baiyun Sag using gray clustering method. Nat Hazards 74:1179–1190. https://doi.org/10.1007/s11069-014-1241-1
Li J, Duan P, Sheng Y (2015) Lv H (2015) Spatial interpolation approach based on IDW with anisotropic spatial structures. Int Conf Intell Earth Obs Appl 9808:98081O. https://doi.org/10.1117/12.2209321
Li B, Jia Y, Liu JP, Liu X, Wang Z (2020) Effect of wave, current, and lutocline on sediment resuspension in Yellow River Delta-Front. Water 12(3):845. https://doi.org/10.3390/w12030845
Liu Z, Jeng DS, Chan AHC, Luan M (2009) Wave-induced progressive liquefaction in a poro-elastoplastic seabed: A two-layered model. Int J Numer Anal Meth Geomech 33:591–610. https://doi.org/10.1002/nag.734
Liu X, Jia Y, Zheng J, Wen M, Shan H (2017a) An experimental investigation of wave-induced sediment responses in a natural silty seabed: New insights into seabed stratification. Sedimentology 64:508–529. https://doi.org/10.1111/sed.12312
Liu X, Zhang M, Zhang H, Jia Y, Zhu C, Shan H (2017b) Physical and mechanical properties of loess discharged from the Yellow River into the Bohai Sea, China. Eng Geol 227:4–11. https://doi.org/10.1016/j.enggeo.2017.04.019
Liu X, Zhu C, Zheng J, Guo L, Yin P, Jia Y (2017c) The observations of seabed sediment erosion and resuspension processes in the Jiaozhou Bay in China. Acta Oceanol Sin 36(11):79–85. https://doi.org/10.1007/s13131-016-1072-5
Liu X, Zheng J, Hong Z, Zhang S, Liu B, Shan H, Jia Y (2018) Sediment critical shear stress and geotechnical properties along the modern Yellow River Delta, China. Mar Georesour Geotechnol 36(8):875–882. https://doi.org/10.1080/1064119X.2017.1393477
Liu X, Zhang S, Zheng J, Zhang H, Jia Y (2019) Experimental dynamic sediment behavior under storm waves with a 50 year recurrence interval in the Yellow River Delta. Anthropocene Coasts 2:229–243. https://doi.org/10.1139/anc-2018-0018
Liu X, Zhang H, Zheng J, Guo L, Jia Y, Bian C, Li M, Ma L, Zhang S (2020) Critical role of wave-seabed interactions in the extensive erosion of Yellow River estuarine sediments. Mar Geol 426:106208. https://doi.org/10.1016/j.margeo.2020.106208
Liu X, Yang Q, Wang Y, Jeng D, Sturm H (2021) New advances in marine engineering geology. J Mar Sci Eng 9(1):66. https://doi.org/10.3390/books978-3-0365-2422-1
Liu X, Lu Y, Yu H, Ma L, Li X, Li W, Zhang H, Bian C (2022) In-situ observation of storm-induced wave-supported fluid mud occurrence in the subaqueous Yellow River delta. J Geophys Res Oceans 127(7):e2021JC018190. https://doi.org/10.1029/2021JC018190
Locat J, Lee HJ (2002) Submarine landslides: advances and challenges. Can Geotech J 39(1):193–212. https://doi.org/10.1139/t01-089
Lu F, Zhang H, Jia Y, Liu W, Wang H (2019) Migration and diffusion of heavy metal Cu from the interior of sediment during wave-induced sediment liquefaction process. J Mar Sci Eng 7(12):449. https://doi.org/10.3390/jmse7120449
Lukasz L, Joanna K (2021) Life cycle assessment of opencast lignite mining. Int J Coal Sci Technol 8(6):1272–1287. https://doi.org/10.1007/s40789-021-00467-9
Madsen OS (1978) Wave-induced pore pressures and effective stresses in a porous bed. Geotechnique 28(4):377–393. https://doi.org/10.1680/geot.1978.28.4.377
Maloney JM, Bentley SJ, Xu K, Obelcz J, Georgiou YI, Jafari NH, Miner MD (2020) Mass wasting on the Mississippi River subaqueous delta. Earth-Sci Rev 200:103001. https://doi.org/10.1016/j.earscirev.2019.103001
Mandal S, Patil SG, Manjunatha YR, Hegde AV (2008) Application of neural networks in coastal engineering—an overview. Paper presented at the 12th international conference on computer methods and advances in geomechanics (IACMAG), Goa, India, 1–6 October 2008
Marques F, Matildes R, Redweik P (2013) Statistically based sea cliff instability susceptibility assessment at regional scale, at the Burgau-Lagos Coastal Section (Algarve, Portugal). In: Margottini C (ed) Landslide science and practice. Springer, Berlin, pp 147–153
McAdoo BG, Pratson LF, Orange DL (2000) Submarine landslide geomorphology, US continental slope. Mar Geol 169(1–2):103–136. https://doi.org/10.1016/S0025-3227(00)00050-5
Mersha T, Meten M (2020) GIS-based landslide susceptibility mapping and assessment using bivariate statistical methods in Simada area, northwestern Ethiopia. Geoenviron Disasters 7:20. https://doi.org/10.1186/s40677-020-00155-x
Meunier P, Hovius N, Haines AJ (2007) Regional patterns of earthquake-triggered landslides and their relation to ground motion. Geophys Res Lett 34:L20408. https://doi.org/10.1029/2007GL031337
Mitchell NC (2003) Susceptibility of mid-ocean ridge volcanic islands and seamounts to large-scale landsliding. J Geophys Res Solid Earth 108:2397. https://doi.org/10.1029/2002JB001997
Nataraja MS, Harbinder SG (1983) Ocean wave-induced liquefaction analysis. J Geotech Eng 109(1983):573–590. https://doi.org/10.1061/(ASCE)0733-9410(1983)109:4(573)

Nian T, Guo X, Zheng D, Xiu Z, Jiang Z (2019) Susceptibility assessment of regional submarine landslides triggered by seismic actions. Appl Ocean Res 93:101964. https://doi.org/10.1016/j.apor.2019.101964
Nian T, Song L, Zhao W, Jiao H, Guo X (2022) Submarine slope failure due to overpressure fluid associated with gas hydrate dissociation. Environ Geotech 9(2):108–123. https://doi.org/10.1680/jenge.19.00070
Okusa S (1985) Measurements of wave-induced pore pressure in submarine sediments under various marine conditions. Mar Geotechnol 6(2):119–144. https://doi.org/10.1080/10641198509388184
Owen G (1987) Deformation processes in unconsolidated sands. Geol Soc Lond Special Publ 29(1):11–24. https://doi.org/10.1144/GSL.SP.1987.029.01.02
Phillips SJ, Dudík M (2008) Modeling of species distributions with Maxent: new extensions and a comprehensive evaluation. Ecography 31(2):161–175. https://doi.org/10.1111/j.0906-7590.2008.5203.x
Phillips SJ, Anderson RP, Schapire RE (2006) Maximum entropy modeling of species geographic distributions. Ecol Model 190(3–4):231–259. https://doi.org/10.1016/j.ecolmodel.2005.03.026
Pietruszczak S, Pande GN (1996) Constitutive relations for partially saturated soils containing gas inclusions. J Geotech Eng 122(1):50–59. https://doi.org/10.1061/(ASCE)0733-9410(1996)122:1(50)
Rahman MS (1991) Wave-induced instability of seabed: mechanism and conditions. Mar Geotechnol 10(3–4):277–299. https://doi.org/10.1080/10641199109379896
Rasyid AR, Bhandary NP, Yatabe R (2016) Performance of frequency ratio and logistic regression model in creating GIS based landslides susceptibility map at Lompobattang Mountain, Indonesia. Geoenviron Disasters 3:19. https://doi.org/10.1186/s40677-016-0053-x
Reichenbach P, Rossi M, Malamud BD, Mihir M, Guzzetti F (2018) A review of statistically-based landslide susceptibility models. Earth Sci Rev 180:60–91. https://doi.org/10.1016/j.earscirev.2018.03.001
Saaty TL (1977) A scaling method for priorities in hierarchical structures. J Math Psychol 15(3):234–281. https://doi.org/10.1016/0022-2496(77)90033-5
Saaty TL (1990) How to make a decision: the analytic hierarchy process. Eur J Oper Res 48(1):9–26. https://doi.org/10.1016/0377-2217(90)90057-I
Scarselli N (2020) Submarine landslides–architecture, controlling factors and environments. A summary. In: Scarselli N (eds) Principles of geologic analysis. Regional Geology and Tectonics (Second Edition), vol 1. Elsevier. pp 417–439
Seed HB, Izzat MI (1971) Simplified procedure for evaluating soil liquefaction potential. J Soil Mech Found 97(9):1249–1273. https://doi.org/10.1061/JSFEAQ.0001662
Shan Z, Wu H, Ni W, Sun M, Wang K, Zhao L, Lou Y, Liu A, Xie W, Zheng X, Guo X (2022) Recent technological and methodological advances for the investigation of submarine landslides. J Mar Sci Eng 10(11):1728. https://doi.org/10.3390/jmse10111728
Shanmugam G, Wang Y (2015) The landslide problem. J Palaeogeogr 4(2):109–166. https://doi.org/10.3724/SP.J.1261.2015.00071
Shano L, Raghuvanshi TK, Meten M (2020) Landslide susceptibility evaluation and hazard zonation techniques—a review. Geoenviron Disasters 7:18. https://doi.org/10.1186/s40677-020-00152-0
Song B, Cheng Y, Yan C, Han Z, Ding J, Li Y, Wei J (2019) Influences of hydrate decomposition on submarine landslide. Landslides 16:2127–2150. https://doi.org/10.1007/s10346-019-01217-4
Sultan N, Cochonat P, Canals M, Cattaneo A, Dennielou B, Haflidason H, Laberg JS, Long D, Mienerte J, Trincardic F, Urgelesb R, Vorrene TO, Wilson C (2004a) Triggering mechanisms of slope instability processes and sediment failures on continental margins: a geotechnical approach. Mar Geol 213(1–4):291–321. https://doi.org/10.1016/j.margeo.2004.10.011
Sultan N, Cochonat P, Foucher JP, Mienert J (2004b) Effect of gas hydrates melting on seafloor slope instability. Mar Geol 213(1–4):379–401. https://doi.org/10.1016/j.margeo.2004.10.015
Sultan N (2007) Excess pore pressure and sediment deformation resulting from gas-hydrates dissociation and dissolution. In Offshore technology conference. Houston, TX, 18532. DOI: https://doi.org/10.4043/18532-MS
Sumer BM, Fredsøe J, Christensen S, Lind MT (1999) Sinking/floatation of pipelines and other objects in liquefied soil under waves. Coast Eng 38(2):53–90. https://doi.org/10.1016/S0378-3839(99)00024-1
Sumer BM, Ansal A, Cetin KO, Damgaard J, Gunbak AR, Hansen NO, Sawicki A, Synolakis CE, Yalciner AC, Yuksel Y, Zen K (2007) Earthquake-induced liquefaction around marine structures. J Waterw Port Coast Ocean Eng 133(1):55–82. https://doi.org/10.1061/(ASCE)0733-950X(2007)133:1(55)
Talling PJ, Clare M, Urlaub M, Pope E, Hunt JE, Watt SFL (2014) Large submarine landslides on continental slopes: geohazards, methane release, and climate change. Oceanography 27(2):32–45. https://doi.org/10.5670/oceanog.2014.38
Ulker MBC, Rahman MS (2009) Response of saturated and nearly saturated porous media: different formulations and their applicability. Int J Numer Anal Meth Geomech 33(5):633–664. https://doi.org/10.1002/nag.739
Urgeles R, Camerlenghi A (2013) Submarine landslides of the Mediterranean Sea: trigger mechanisms, dynamics, and frequency-magnitude distribution. J Geophys Res Earth Surf 118:2600–2618. https://doi.org/10.1002/2013JF002720
Uri S, Lee HJ, Geist EL, Twichell D (2009) Assessment of tsunami hazard to the US East Coast using relationships between submarine landslides and earthquakes. Mar Geol 264(1–2):65–73. https://doi.org/10.1016/j.margeo.2008.05.011
Van Westen CJ (1997) Statistical landslide hazard analysis. ILWIS 2.1 for Windows application guide. ITC Publication, Enschede, pp 73–84
Wang H, Liu G, Xu W, Wang G (2005) GIS-based landslide hazard assessment: an overview. Prog Phys Geogr 29(4):548–567. https://doi.org/10.1191/0309133305pp462ra
Wang H, Zhang R, Liu W, Liu K, Wang G (2011) Kriging interpolation method optimized by support vector machine and its application in oceanic data. Trans Atmosp Sci 34(5):567–573. https://doi.org/10.13878/j.cnki.dqkxxb.2011.05.014. (**in Chinese with English abstract**)
Wang Z, Jia Y, Liu X, Dong W, Shan H, Guo L, Wei W (2018) In situ observation of storm-wave-induced seabed deformation with a submarine landslide monitoring system. Bull Eng Geol Environ 77:1091–1102. https://doi.org/10.1007/s10064-017-1130-4
Wang L, Rui S, Guo Z, Gao Y, Zhou W, Liu Z (2020a) Seabed trenching near the mooring anchor: history cases and numerical studies. Ocean Eng 218:108233. https://doi.org/10.1016/j.oceaneng.2020.108233
Wang Z, Sun Y, Jia Y, Shan Z, Shan H, Zhang S, Wen M, Liu X, Song Y, Zhao D, Wen S (2020b) Wave-induced seafloor instabilities in the subaqueous Yellow River Delta—initiation and process of sediment failure. Landslides 17:1849–1862. https://doi.org/10.1007/s10346-020-01399-2
Wang Y, Wang R, Zhang J (2021) Large-scale seismic seafloor stability analysis in the South China Sea. Ocean Eng 235:109334. https://doi.org/10.1016/j.oceaneng.2021.109334
Wen M, Shan H, Zhang S, Liu L, Jia Y (2019) Contribution of waves and currents to sediment resuspension in the Yellow River Delta. Mar Georesour Geotechnol 37(1):96–102. https://doi.org/10.1080/1064119X.2018.1452084
Wen L, Zhang L, Bai J, Wang Y, Wei Z, Liu H (2022) Optimizing spatial interpolation method and sampling number for predicting cadmium distribution in the largest shallow lake of North China. Chemosphere 309(2):136789. https://doi.org/10.1016/j.chemosphere.2022.136789
Xu J, Zhang M, Fan W (2015) An overview of geological disaster risk assessment. J Catastrophol 30(4):130–134 (**in Chinese**)
Xu X, Xu G, Yang J, Xu Z, Ren Y (2021) Field observation of the wave-induced pore pressure response in a silty soil seabed. Geo-Mar Lett 41:13. https://doi.org/10.1007/s00367-020-00680-6
Xu H, Su P, Chen Q, Liu F, Zhou Q, Liu L (2022) Susceptibility areas identification and risk assessment of debris flow using the Flow-R model: a case study of Basu County of Tibet. Geoenviron Disasters 9:13. https://doi.org/10.1186/s40677-022-00216-3
Yang Z, Yu X, Dedman S, Rosso M, Ja Z, Yang J, Xia Y, Tian Y, Zhang G, Wang J (2022) UAV remote sensing applications in marine monitoring: Knowledge visualization and review. Sci Total Environ 838(1):155939. https://doi.org/10.1016/j.scitotenv.2022.155939
Ye Y et al (2017b) Chapter 3—classification of marine hazard geology factors and marine geological hazards. In: Ye Y (ed) Marine geo-hazards in China. Elsevier, Amsterdam, pp 77–87. https://doi.org/10.1016/B978-0-12-812726-1.00003-6
Ye Y et al (2017a) Introduction. In: Ye Y (Eds.) Marine geo-hazards in China. Amsterdam: Elsevier, pp 1–34. DOI: https://doi.org/10.1016/B978-0-12-812726-1.00001-2
Youd T, Perkins D (1978) Mapping liquefaction-induced ground failure potential. J Geotech Eng Div 104(4):433–446. https://doi.org/10.1061/AJGEB6.0000612

Youd TL, Idriss IM, Andrus RD, Arango I, Castro G, Christian JT, Dobry R, Finn WDL, Harder LF, Hynes ME, Ishihara K, Koester JP, Liao SSC, Marcuson WF, Martin GR, Mitchell JK, Martin GR, Mitchell JK, Moriwaki Y, Power MS, Robertson PK, Seed RB, Stokoe KH (2001) Liquefaction resistance of soils: summary report from the 1996 NCEER and 1998 NCEER/NSF workshops on evaluation of liquefaction resistance of soils. J Geotech Geoenviron Eng 127(10):817–833. https://doi.org/10.1061/(ASCE)1090-0241(2001)127:10(817)

Yu H, Liu L, Lu Y, Li W, Gao H, Wu R, Li X (2022) Characteristics of the sediment gravity flow triggered by wave-induced liquefaction on a sloping silty seabed: an experimental investigation. Front Earth Sci 10:909605. https://doi.org/10.3389/feart.2022.909605

Yu P, Liu H, Wang Z, Fu J, Zhang H, Wang J, Yang Q (2023) Development of urban underground space in coastal cities in China: a review. Deep Undergr Sci Eng. https://doi.org/10.1002/dug2.12034

Zahedi F (1986) The analytic hierarchy process: a survey of the method and its applications. Interfaces 16(4):96–108. https://doi.org/10.1287/inte.16.4.96

Zare A, Hoboubi N, Farahbakhsh S, Jahangiri M (2022) Applying analytic hierarchy process and failure likelihood index method (AHP-FLIM) to assess human reliability in critical and sensitive jobs of a petrochemical industry. Heliyon 8(5):e09509. https://doi.org/10.1016/j.heliyon.2022.e09509

Zen K, Yamazaki H (1990a) Mechanism of wave-induced liquefaction and densification in seabed. Soils Found 30(4):90–104. https://doi.org/10.3208/sandf1972.30.4_90

Zen K, Yamazaki H (1990b) Oscillatory pore pressure and liquefaction in seabed induced by ocean waves. Soils Found 30(4):147–161. https://doi.org/10.3208/sandf1972.30.4_147

Zen K, Yamazaki H (1991) Field Observation and analysis of wave-induced liquefaction in seabed. Soils Found 31(4):161–179. https://doi.org/10.3208/sandf1972.31.4_161

Zhang L, Luan X (2012) Quantitative analysis of submarine slope stability on the northern of the South China Sea. Prog Geophys 27(4):1443–1453 (**in Chinese**)

Zhang Y, Jeng DS, Gao FP, Zhang JS (2013) An analytical solution for response of a porous seabed to combined wave and current loading. Ocean Eng 57:240–247. https://doi.org/10.1016/j.oceaneng.2012.09.001

Zhang M, Huang Y, Bao Y (2016) The mechanism of shallow submarine landslides triggered by storm surge. Nat Hazards 81:1373–1383. https://doi.org/10.1007/s11069-015-2112-0

Zhang S, Jia Y, Lu F, Zhang Y, Zhang S, Shan H (2018) Influence of seepage flows on the erodibility of fluidized silty sediments: parameterization and mechanisms. J Geophys Res Oceans 123(5):3307–3321. https://doi.org/10.1002/2018JC013805

Zhang J, Song S, Zhai Y, Tong L, Guo Y (2019a) Numerical study on the wave-induced seabed response around a trenched pipeline. J Coastal Res 35(4):896–906. https://doi.org/10.2112/JCOASTRES-D-18-00135.1

Zhang S, Jia Y, Lu F, Zhang Y, Zhang S, Peng Z (2019b) Effects of upward seepage on the resuspension of consolidated silty sediments in the yellow river delta. J Coastal Res 36(2):372–381. https://doi.org/10.2112/JCOASTRES-D-18-00162.1

Zhang H, Liu X, Jia Y, Du Q, Sun Y, Yin P, Shan H (2020) Rapid consolidation characteristics of Yellow River-derived sediment: geotechnical characterization and its implications for the deltaic geomorphic evolution. Eng Geol 270:105578. https://doi.org/10.1016/j.enggeo.2020.105578

Zhang H, Liu X, Chen A, Li W, Lu Y, Guo X (2021) Design and application of an in situ test device for rheological characteristic measurements of liquefied submarine sediments. J Mar Sci Eng 9(6):639. https://doi.org/10.3390/jmse9060639

Zhang X, Li L, Xu C (2022) Large-scale landslide inventory and their mobility in Lvliang City, Shanxi Province, China. Nat Hazards Res 2(2):111–120. https://doi.org/10.1016/j.nhres.2022.05.002

Zheng J, Jia Y, Liu X, Shan H, Zhang M (2013) Experimental study of the variation of sediment erodibility under wave-loading conditions. Ocean Eng 68:14–26. https://doi.org/10.1016/j.oceaneng.2013.04.010

Zhou J, Chen C, Wang M, Khandelwal M (2021) Proposing a novel comprehensive evaluation model for the coal burst liability in underground coal mines considering uncertainty factors. Int J Min Sci Technol 31(5):799–812. https://doi.org/10.1016/j.ijmst.2021.07.011

Zhu C, Jia Y, Liu X, Zhang H, Wen M, Huang M, Shan H (2015) Classification and genetic mechanism of submarine landslide: a review. Mar Geol Quat Geol 35(6):153–164. https://doi.org/10.16562/j.cnki.0256-1492.2015.06.016. (**in Chinese**)

Zhu B, Pei H, Yang Q (2018) Probability analysis of submarine landslides based on the response surface method: a case study from the South China Sea. Appl Ocean Res 78:167–179. https://doi.org/10.1016/j.apor.2018.06.018

Publisher's Note